

Multivariable evolution in final state parton shower algorithms

Zoltán Nagy

Deutsches Elektronen-Synchrotron DESY, Notkestr. 85, 22607 Hamburg, Germany *

Davison E. Soper

Institute for Fundamental Science, University of Oregon, Eugene, OR 97403-5203, USA †

(Dated: 19 January 2022)

One can use more than one scale variable to specify the family of surfaces in the space of parton splitting parameters that define the evolution of a parton shower. Considering e^+e^- annihilation, we use two variables, with shower evolution following a special path in this two dimensional space. In addition, we treat in a special way the part of the splitting function that has a soft emission singularity but no collinear singularity. This leads to certain advantages compared to the usual shower formulation with only one scale variable.

Keywords: perturbative QCD, parton shower

I. INTRODUCTION

In a parton shower event generator, one can view the parton state as evolving according to an operator based renormalization group equation. Starting with a state with just a few partons, the shower evolves as a scale μ_s changes from a large value μ_H characteristic of the hard scattering state at the start of the shower to a low value μ_f on the order of 1 GeV. As the shower evolves, more and more partons are emitted. The function of the shower scale μ_s is to divide possible parton splittings into *resolvable* splittings, with scales $\mu > \mu_s$, and *unresolvable* splittings, with scales $\mu < \mu_s$. There is substantial freedom to choose exactly what this means. The space of possible splittings is divided into the resolvable and unresolvable regions by a surface labelled by μ_s . Many different choices are possible for defining this surface. For instance, one can use a measure of the transverse momentum in the splitting to define the surface or one can use a measure of the virtuality in the splitting.

In this paper, we explore the possibility of using more than one variable to define a family of surfaces. Instead of one μ_s , we use $\vec{\mu} = (\mu_1, \mu_2, \dots)$. Then evolution means moving from large values of the component scales μ_n to small values along a path $\vec{\mu}(t)$ with $0 < t < \infty$. Defining this path is then part of defining the shower algorithm.

There is an additional freedom available when multiple scales are involved. It may be possible to divide the shower splitting functions into separate terms such that one of the terms is not sensitive to one of the scales in the sense that no singularity is encountered when this scale approaches zero. When this happens, we can modify the definition of the unresolved region for this term in a way that makes this term exactly independent of this scale. This redefinition can simplify the shower evolution.

In this paper, we explore the additional freedom obtained by using two scales instead of one.

This general concept works for proton-proton, e^\pm -proton, and e^+e^- collisions. The simplest case is e^+e^- collisions, so we consider e^+e^- collisions in this paper, reserving cases involving incoming hadrons for future work.

We begin in Secs. II and III with a general description of multivariable evolution in the framework of shower splittings defined at any order of perturbation theory and matched to perturbative QCD at any order of perturbation theory [1]. This will help us to understand the path dependence in general. In existing parton shower programs [2–5], including ours [6–18], the shower splitting operators are only defined at order α_s^1 , although some higher order contributions may be included by adjusting the scale argument of α_s .

In Sec. IV, we turn to parton splitting operators truncated to order α_s^1 , possibly with more than one scale. Then in Sec. V, we define the unresolved region for first order splittings with one scale, based either on transverse momentum or on virtuality or on angle. In Sec. VI we generalize this to two scales. One of these scales is one of the previously considered scales based on transverse momentum, virtuality, or angle. We make a specific useful choice for the second scale, a special choice for the unresolved region for part of the splitting operator, and a corresponding specific choice for the path. In Sec. VII, we examine the form of shower evolution in this scheme. In particular, we find that this gives us a different way of understanding an angular ordered shower within the context of the general formalism of Ref. [1]. In Sec. VIII, we find that the choices made in the previous sections give us a substantially improved treatment of SU(3) color within the context of a first order parton shower. In Sec. IX, we discuss the possibility of a more complex path $\vec{\mu}(t)$ within the two scale space previously defined. In Sec. X, we provide a numerical example for e^+e^- annihilation at 10 TeV. Finally, we provide a short summary in Sec. XI. There are two appendices, A with details about kinematics and splitting functions and B with some results about the summation of large logarithms.

* Zoltan.Nagy@desy.de

† soper@uoregon.edu

II. GENERAL STRUCTURE OF UNRESOLVED REGIONS

This paper generally concerns the definition of the unresolved region in the space of parton momenta in a parton shower. We will concentrate in the following sections on a single emission in a first order shower, but we begin with a discussion of the general case of a shower algorithm at an arbitrary order of perturbation theory. We use the general framework presented in Ref. [1]. This general framework allows for substantial freedom in choosing the functions that define a particular parton shower algorithm. We have developed particular realizations of these choices for a first order shower [6]. It remains an open problem to realize these choices for a parton shower with splitting functions beyond order α_s . The general theory applies to hadron-hadron collisions, lepton-hadron collisions, and e^+e^- collisions, but in this paper we restrict our analysis to e^+e^- annihilation so as to present the methods that we have in mind in the simplest possible context.

Denote by Q the total momentum of the electron and positron. At some stage in the shower, there are m partons with momenta and flavors $\{p, f\}_m = \{p_1, f_1; p_2, f_2, \dots, p_m, f_m\}$, with

$$\sum_{i=1}^m p_i = Q. \quad (1)$$

We consider operators that create parton splittings and the exchange of virtual partons. After the action of one of these operators, we have partons with momenta and flavors $\{\hat{p}, \hat{f}\}_{\hat{m}}$ with $\hat{m} \geq m$. Momentum is conserved, so that

$$\sum_{i=1}^{\hat{m}} \hat{p}_i = Q. \quad (2)$$

The general theory is expressed using linear operators that act on a vector space that we call the statistical space. Basis vectors for this space have the form $|\{p, f, c, c', s, s'\}_m\rangle$. Here (c, c') and (s, s') represent the quantum colors and spins of the m partons. We use the apparatus of quantum statistical mechanics, with the

color and spin part of $|\{p, f, c, c', s, s'\}_m\rangle$ representing the density matrix $|\{c, s\}_m\rangle\langle\{c', s'\}_m|$.

The general theory of Ref. [1] is based on what is called the infrared sensitive operator $\mathcal{D}(\mu_R^2, \mu_S^2)$. Here μ_R is the standard renormalization scale and μ_S is called the shower scale. In this paper, we contemplate the possibility of having more than one independent shower scale, $\vec{\mu} = (\mu_1, \mu_2, \dots)$. The infrared sensitive operator is expanded in operators $\mathcal{D}^{(n_R, n_V)}(\mu_R, \vec{\mu})$,

$$\mathcal{D}(\mu_R, \vec{\mu}) = 1 + \sum_{n=1}^k \left[\frac{\alpha_s(\mu_R^2)}{2\pi} \right]^n \sum_{n_R=0}^n \sum_{n_V=0}^n \mathcal{D}^{(n_R, n_V)}(\mu_R, \vec{\mu}). \quad (3)$$

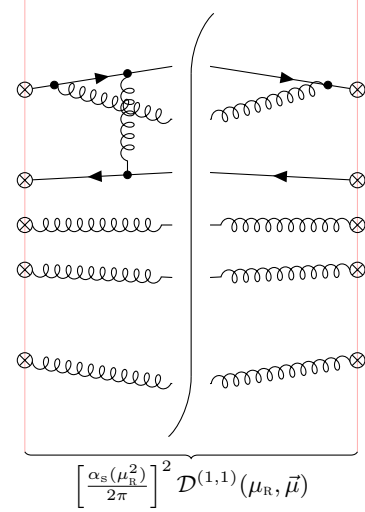


FIG. 1. A contribution to $\mathcal{D}^{(1,1)}$. The partons next to the final state cut are on shell with momenta $\{\hat{p}\}_{m+1}$ and spins $\{\hat{s}\}_{m+1}$ on the left and $\{s'\}_{m+1}$ on the right. At the \otimes symbols, some of the parton lines are off shell propagators. The \otimes vertices connect these propagators to partons with momenta $\{p\}_m$ and spins $\{s\}_m$ on the left and $\{s'\}_m$ on the right.

The operator $\mathcal{D}^{(n_R, n_V)}(\mu_R, \vec{\mu})$ creates n_R real emissions and n_V virtual exchanges. An example graph for $\mathcal{D}^{(1,1)}$ is illustrated in Fig. 1.

We propose a straightforward structure for the operator $\mathcal{D}^{(n_R, n_V)}$:

$$\begin{aligned} & \langle \{\hat{p}, \hat{f}, \hat{c}, \hat{c}', \hat{s}, \hat{s}'\}_{m+n_R} | \mathcal{D}^{(n_R, n_V)}(\mu_R, \vec{\mu}) | \{p, f, c, c', s, s'\}_m \rangle \\ &= \sum_{G \in \text{Graphs}} \sum_{I \in \text{Terms}(G)} \int d^d \{\ell\}_{n_V} \langle \{\hat{p}, \hat{f}\}_{m+n_R} | \mathcal{P}(G, I) | \{p, f\}_m \rangle \\ & \quad \times \langle \{\hat{c}, \hat{s}\}_{m+n_R} | \mathbf{V}_L(G, I; \{\hat{p}, \hat{f}\}_{m+n_R}, \{\ell\}_{n_V}, \mu_R) | \{c, s\}_m \rangle \\ & \quad \times \langle \{c, s\}_m | \mathbf{V}_R^\dagger(G, I; \{\hat{p}, \hat{f}\}_{m+n_R}, \{\ell\}_{n_V}, \mu_R) | \{\hat{c}, \hat{s}\}_{m+n_R} \rangle_D \\ & \quad \times \Theta(G, I; \{\hat{p}, \hat{f}\}_{m+n_R}, \{\ell\}_{n_V}; \vec{\mu}). \end{aligned} \quad (4)$$

There are n_v virtual exchanges, so there is an integration over the space of loop momenta ℓ for these exchanges. There is a sum over Feynman graphs like that in Fig. 1. It may be desirable to break the Feynman graphs into separate terms with different sorts of singularity structures. For this reason, there is a sum over terms I of each graph. The factor $(\{\hat{p}, \hat{f}\}_{m+n_r} | \mathcal{P}(G, I) | \{p, f\}_m)$ consists of delta functions that fix $\{p, f\}_m$ in terms of $\{\hat{p}, \hat{f}\}_{m+n_r}$ according to the momentum mapping chosen for the shower, as in Appendix A at first order. The effects of the graphs acting on the ket state (L) and the bra state (R) are encoded in \mathbf{V}_L and \mathbf{V}_R^\dagger , which are operators on the quantum color and spin space.¹ An example at first order is worked out in Ref. [6], while providing examples beyond first order remains an open problem.

The final factor in Eq. (4) is of most interest for this paper. It defines the unresolved region. The parton splitting functions \mathbf{V}_L and \mathbf{V}_R^\dagger are singular in a surface in the space of momenta $\{\{\hat{p}\}_{m+n_r}, \{\ell\}_{n_v}\}$ in which some of the momenta are exactly collinear to each other or some are zero. We illustrate this singular surface conceptually by the red lines in Fig. 2. The unresolved region is a region in the space of momenta that surrounds the singular surface. We illustrate this unresolved region by the blue area in Fig. 2. The singular surface must not extend outside of the unresolved region. That is, to borrow a phrase from general relativity, there can be *no naked singularity*. The idea behind this is that a measurement using an infrared safe measurement algorithm (such as a jet algorithm) cannot distinguish between a single parton and a set partons, some of which carry very small momenta and the others of which carry momenta that are very nearly collinear. One can then say that the difference between these two states is unresolvable. The parton shower version of an unresolvable region incorporates this idea without referring to any specific infrared safe observable. In designing a shower algorithm, there is then great freedom in choosing the unresolved region. We let the boundary of the unresolved region depend on one or more scale parameters $\mu_{s,i}$ such that increasing any of the $\mu_{s,i}$ makes the unresolved region larger and decreasing $\mu_{s,i}$ makes the unresolved region smaller. The function $\Theta(G, I; \{\hat{p}, \hat{f}\}_{m+n_r}, \{\ell\}_{n_v}; \vec{\mu})$, equals 1 when $\{\{\hat{p}\}_{m+n_r}, \{\ell\}_{n_v}\}$ is in the unresolved region and equals 0 otherwise. The complement of the unresolved region is the resolved region, colored yellow in Fig. 2.

III. MULTIPLE SHOWER SCALES

With multiple shower scales $\vec{\mu}$, the singular operator depends on these scales and on the renormalization scale

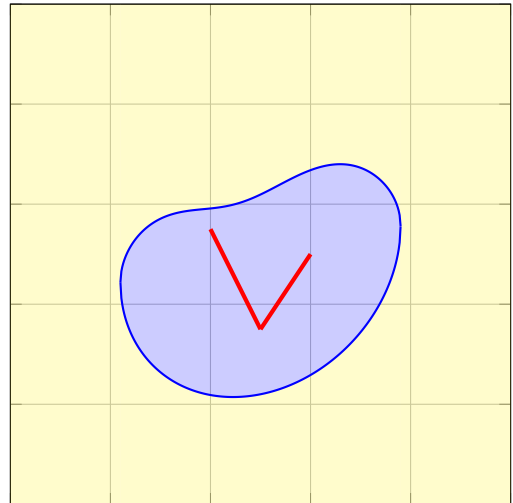


FIG. 2. Resolved and unresolved regions. The red lines represent the singularities. The unresolved region for the momenta is the blue region.

μ_R . We can let the renormalization scale μ_R be some function of the shower scales,²

$$\mu_R = \mu_R(\vec{\mu}). \quad (5)$$

Then we can simplify the notation by writing

$$\mathcal{D}(\vec{\mu}) = \mathcal{D}(\mu_R(\vec{\mu}), \vec{\mu}). \quad (6)$$

The shower will evolve from hard scales $\vec{\mu}_h$ that are characteristic of the hard scattering that initiates the shower to soft scales $\vec{\mu}_f$ that are on the order of 1 GeV.

For e^+e^- annihilation, we define the shower evolution operator by

$$\mathcal{U}(\vec{\mu}_2, \vec{\mu}_1) = \mathcal{D}^{-1}(\vec{\mu}_2) \mathcal{D}(\vec{\mu}_1). \quad (7)$$

We should note that this is special to e^+e^- annihilation. For hadron-hadron collisions, there are initial state singularities and we need parton distribution functions. Then there is a mismatch between the evolution equation for the parton distribution functions and the shower evolution. This mismatch requires the introduction of an operator \mathcal{V} that accounts for threshold logarithms [1, 12, 13]. For e^+e^- annihilation, one can arrange that $\mathcal{V} = 1$. We will return to the analysis of multiple scale evolution for hadron-hadron collisions in a later paper. In this paper, we restrict the analysis to e^+e^- annihilation.

¹ The subscripts D denote dual basis vectors, ${}_D \langle c' s' | c, s \rangle = \delta_{c',c} \delta_{s',s}$ [6].

² In a first order shower, one can modify the shower splitting functions by adjusting the argument of α_s to be not μ_R^2 but an approximation to k_T^2 . This is intended to incorporate terms from higher order splitting functions into the first order splitting function, but it is separate from the general formalism discussed here.

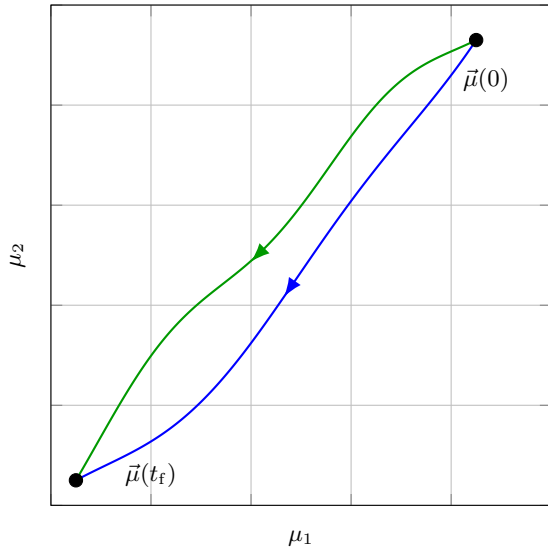


FIG. 3. Two paths in the space of scales from $\vec{\mu}(0)$ to $\vec{\mu}(t_f)$.

Using Eq. (7), to go from the hard scales to the final soft scales we have

$$\mathcal{U}(\vec{\mu}_f, \vec{\mu}_H) = \mathcal{D}^{-1}(\vec{\mu}_f) \mathcal{D}(\vec{\mu}_H). \quad (8)$$

We choose a path $\vec{\mu}(t)$ from $\vec{\mu}_H$ to $\vec{\mu}_f$,

$$\begin{aligned} \vec{\mu}(0) &= \vec{\mu}_H, \\ \vec{\mu}(t_f) &= \vec{\mu}_f. \end{aligned} \quad (9)$$

We define the shower splitting operator

$$\mathcal{S}(t) = -\mathcal{D}^{-1}(\vec{\mu}(t)) \frac{d}{dt} \mathcal{D}(\vec{\mu}(t)). \quad (10)$$

That is

$$\mathcal{S}(t) = -\sum_j \frac{d\mu_j(t)}{dt} \mathcal{S}_j(\vec{\mu}(t)), \quad (11)$$

where

$$\mathcal{S}_j(\vec{\mu}) = \mathcal{D}^{-1}(\vec{\mu}) \frac{\partial}{\partial \mu_j} \mathcal{D}(\vec{\mu}). \quad (12)$$

(Following the notation in Ref. [1] when there is only one shower scale μ , we would have defined $\mu^2(d/d\mu^2)\mathcal{D} = \mathcal{D}\mathcal{S}$, but with more than one scale it is more convenient to use a simple derivative with respect to μ_j .)

Then

$$\frac{d}{dt} \mathcal{U}(\vec{\mu}(t), \vec{\mu}(t_1)) = \mathcal{S}(t) \mathcal{U}(\vec{\mu}(t), \vec{\mu}(t_1)). \quad (13)$$

We can write the solution of this differential equation with boundary condition $\mathcal{U}(\vec{\mu}(t_1), \vec{\mu}(t_1)) = 1$ as

$$\mathcal{U}(\vec{\mu}(t_2), \vec{\mu}(t_1)) = \mathbb{T} \mathcal{U}(t_2, t_1), \quad (14)$$

where, using \mathbb{T} to indicate ordering of operators along the path,

$$\mathcal{U}(t_2, t_1) = \mathbb{T} \exp\left(\int_{t_1}^{t_2} dt \mathcal{S}(t)\right). \quad (15)$$

The operator $\mathcal{U}(t_2, t_1)$ depends on the chosen path. We illustrate schematically the possibility of two paths in Fig. 3 between $\vec{\mu}(0) = \vec{\mu}_H$ and $\vec{\mu}(t_f) = \vec{\mu}_f$. If $\mathcal{S}(t)$ is defined exactly according to Eq. (10), then $\mathcal{U}(t_f, 0)$ does not depend on $\vec{\mu}(t)$ for intermediate values of t , $0 < t < t_f$. This follows simply because of the definition Eq. (7) of \mathcal{U} . However, it is often useful to use an approximation for $\mathcal{S}(t)$, for instance by using only a finite number of terms in its perturbative expansion. If $\mathcal{S}(t)$ is approximated in any way and $\mathcal{U}(t_f, 0)$ is obtained by solving the differential equation (13), then $\mathcal{U}(t_f, 0)$ can depend on the whole path.

To understand the dependence on the path, we can consider an altered path between the same endpoints as illustrated in Fig 3:

$$\mu_j(t; \varepsilon) = \mu_j(t) + \varepsilon \eta_j(t), \quad (16)$$

where

$$\eta_j(0) = \eta_j(t_f) = 0. \quad (17)$$

We can let $\mathcal{U}_\varepsilon(t_f, 0)$ denote the shower evolution operator over the path that has been deformed by an amount ε . We evaluate this operator between the two fixed points at which the deformation vanishes. Then after a little analysis we find

$$\left[\frac{d}{d\varepsilon} \mathcal{U}_\varepsilon(t_f, 0) \right]_{\varepsilon=0} = \int_0^{t_f} dt \mathcal{U}(t_f, t) \sum_{i,j} \frac{d\mu_i(t)}{dt} \eta_j(t) \left[\frac{\partial \mathcal{S}_j(\vec{\mu}(t))}{\partial \mu_i} - \frac{\partial \mathcal{S}_i(\vec{\mu}(t))}{\partial \mu_j} + [\mathcal{S}_i(\vec{\mu}(t)), \mathcal{S}_j(\vec{\mu}(t))] \right] \mathcal{U}(t, 0). \quad (18)$$

The expression in square brackets vanishes if we use

Eq. (12) exactly to define $\mathcal{S}_j(\vec{\mu}(t))$, but not otherwise.

If the perturbative expansion of $S_j(\vec{\mu}(t))$ is truncated at order α_s^N , then the expression in square brackets will be of order α_s^{N+1} .

In this paper, we work with a first order shower, in which the perturbative expansion of $S_j(\vec{\mu}(t))$ is truncated at order α_s^1 . The most straightforward choice of path in the first order shower is computationally difficult because of noncommuting color matrices. We use the freedom to specify a path $\vec{\mu}(t)$ to create a first order shower algorithm that is computationally simpler than with the more straightforward choice of path. The computationally difficult parts of the more straightforward approach are eliminated because, with the chosen path, they would appear only at order α_s^2 .

IV. SPLITTING AT FIRST ORDER

We now turn to the description of the unresolved region for e^+e^- annihilation with total momentum Q in a first order parton shower, such as DEDUCTOR. In the description that we use in this paper, the partons carry color³, but, as in the current version of DEDUCTOR, we average over spins so that there are no spin states represented in the parton states. We begin with m partons, in a state $|\{p, f, c, c'\}_m\rangle$. The singular operator $\mathcal{D}(\vec{\mu})$ has a perturbative expansion

$$\mathcal{D}(\vec{\mu}) = 1 + \mathcal{D}^{[1]}(\vec{\mu}) + \mathcal{O}(\alpha_s^2), \quad (19)$$

where $\mathcal{D}^{[1]}(\vec{\mu})$ contains a factor of α_s ,

$$\mathcal{D}^{[1]}(\vec{\mu}) = \frac{\alpha_s(\mu_R^2(\vec{\mu}))}{2\pi} \mathcal{D}^{(1)}(\vec{\mu}). \quad (20)$$

The operator $\mathcal{D}^{[1]}(\vec{\mu})$ consists of two terms,

$$\mathcal{D}^{[1]}(\vec{\mu}) = \mathcal{D}^{[1,0]}(\vec{\mu}) + \mathcal{D}^{[0,1]}(\vec{\mu}). \quad (21)$$

In $\mathcal{D}^{[1,0]}(\vec{\mu})$ one of the partons splits into two. In $\mathcal{D}^{[0,1]}(\vec{\mu})$, a virtual parton is exchanged, leaving the number of partons unchanged.

In the real emission operator $\mathcal{D}^{[1,0]}(\vec{\mu})$, let l be the label of the parton that splits, so that p_l is its momentum. This splitting produces two partons, which we label l and $m+1$. These partons carry momenta \hat{p}_l and \hat{p}_{m+1} . In DEDUCTOR, the momenta of the other partons after the splitting, \hat{p}_i , are adjusted by means of a small Lorentz transformation so that momentum is conserved, as in Eq. (2). We can describe the splitting by splitting variables (y, z, ϕ) . Here ϕ is the azimuthal angle of \hat{p}_{m+1} about the p_l axis in the rest frame of Q . The momentum fraction z is defined by

$$\frac{1-z}{z} = \frac{\hat{p}_{m+1} \cdot n_l}{\hat{p}_l \cdot n_l}, \quad (22)$$

where the lightlike vector n_l is

$$n_l = \frac{2p_l \cdot Q}{Q^2} Q - p_l. \quad (23)$$

Finally, y is the dimensionless virtuality variable

$$y = \frac{2\hat{p}_l \cdot \hat{p}_{m+1}}{2p_l \cdot Q}. \quad (24)$$

The default ordering variable in DEDUCTOR is Λ^2 , defined by [11]

$$\Lambda^2 = yQ^2 = a_l 2\hat{p}_l \cdot \hat{p}_{m+1}, \quad (25)$$

where a_l is a dimensionless measure of the inverse of the energy of the mother parton,

$$a_l = \frac{Q^2}{2p_l \cdot Q}. \quad (26)$$

Momentum conservation implies that $a_l \geq 1$.

Parton splittings are often described by the squared transverse momentum k_T^2 in the splitting. Then with the kinematic definitions used in DEDUCTOR, as outlined in Appendix A,

$$k_T^2 = \frac{z(1-z)}{a_l} \Lambda^2. \quad (27)$$

We can also describe the parton splitting using the angle variable

$$\vartheta = \frac{1}{2} [1 - \cos(\theta)], \quad (28)$$

where θ is the angle between the daughter parton momenta in the rest frame of Q . That is

$$\vartheta = \frac{\hat{p}_l \cdot \hat{p}_{m+1}}{2\hat{p}_l \cdot Q \hat{p}_{m+1} \cdot Q} Q^2. \quad (29)$$

The variables k_T^2 , Λ^2 , and ϑQ^2 are measures of the hardness of a splitting. We can relate these variables. We relate k_T^2 to Λ^2 using Eq. (27). To relate ϑ to Λ^2 we can use the definition (29),

$$\vartheta Q^2 = a_l \frac{p_l \cdot Q}{\hat{p}_l \cdot Q} \frac{p_l \cdot Q}{\hat{p}_{m+1} \cdot Q} \Lambda^2. \quad (30)$$

For small angle splittings, in which $\hat{p}_l \approx zp_l$ and $\hat{p}_{m+1} \approx (1-z)p_l$, this is

$$\vartheta Q^2 \approx \frac{a_l}{z(1-z)} \Lambda^2. \quad (31)$$

(The exact relationship is in Eq. (37) or Eq. (A10).) Thus Λ^2 lies between k_T^2 and ϑQ^2 : k_T^2 is smaller by a factor $z(1-z)/a_l$ and ϑQ^2 is larger by (approximately) the inverse of this factor.

Let $\mathcal{D}^{[1,0]}(\vec{\mu})$ act on a state with parton momenta and flavors $\{p, f\}_m$. Consider the contribution in

³ We describe the color treatment in somewhat more detail in Sec. VIII.

which parton l splits with splitting variables (y, z, ϕ) and flavor \hat{f}_{m+1} of the emitted parton. This contribution is proportional to an operator that we can call $\mathbf{D}_l(\{\hat{p}, \hat{f}\}_{m+1}; \{p, f\}_m)$. Here \mathbf{D}_l is a function of the momenta and flavors before and after the splitting but is still an operator on the color space of the partons. The relation of $\mathcal{D}^{[1,0]}(\vec{\mu})$ to $\mathbf{D}_l(\{\hat{p}, \hat{f}\}_{m+1}; \{p, f\}_m)$ is outlined in Appendix A.

For e^+e^- annihilation (but not for hadron-hadron collisions), $\mathcal{D}^{[0,1]}(\vec{\mu})$ is determined from $\mathcal{D}^{[1,0]}(\vec{\mu})$ in a simple way [12]. See Appendix A.

We specify $\mathbf{D}_l(\{\hat{p}, \hat{f}\}_{m+1}; \{p, f\}_m)$ in detail in Appendix A, but for now these details do not matter. What is important is that \mathbf{D}_l exhibits collinear and soft singularities. To describe these singularities, it is useful to consider \mathbf{D}_l at fixed $\{p\}_m$ to be a function of the angle variable ϑ , Eq. (29), and the momentum fraction z , Eq. (22). Then \mathbf{D}_l is singular in the collinear limit, $\vartheta \rightarrow 0$ with fixed z , in the soft limit $(1-z) \rightarrow 0$ with fixed ϑ , and in the soft \times collinear limit, $(1-z) \rightarrow 0$ and $\vartheta \rightarrow 0$. It is of some significance that \mathbf{D}_l can be decomposed into two terms,

$$\begin{aligned} \mathbf{D}_l(\{\hat{p}, \hat{f}\}_{m+1}; \{p, f\}_m) &= \mathbf{D}_l^{\text{sc}}(\{\hat{p}, \hat{f}\}_{m+1}; \{p, f\}_m) \\ &\quad + \mathbf{D}_l^{\text{soft}}(\{\hat{p}, \hat{f}\}_{m+1}; \{p, f\}_m), \end{aligned} \quad (32)$$

where \mathbf{D}_l^{sc} has both soft and collinear singularities, while $\mathbf{D}_l^{\text{soft}}$ has a soft singularity but no collinear singularity (and no soft \times collinear singularity). An example of such a decomposition will be given in Eq. (57). The decomposition of \mathbf{D}_l leads to a corresponding decomposition of $\mathcal{D}^{[1,0]}(\vec{\mu})$,

$$\mathcal{D}^{[1,0]}(\vec{\mu}) = \mathcal{D}_{\text{sc}}^{[1,0]}(\vec{\mu}) + \mathcal{D}_{\text{soft}}^{[1,0]}(\vec{\mu}). \quad (33)$$

$$a_{\perp}(z, k_{\text{T}}^2) = \begin{cases} \frac{a_l^2 k_{\text{T}}^2 / Q^2}{z(1-z) + a_l k_{\text{T}}^2 / Q^2 + a_l^2 (1-4z(1-z)) k_{\text{T}}^2 / Q^2} & \text{for } z(1-z) > c_z k_{\text{T}}^2 / Q^2 \\ 1 & \text{otherwise} \end{cases}. \quad (37)$$

Here a_l was defined in Eq. (26) and

$$c_z = a_l (\sqrt{a_l} + \sqrt{a_l - 1})^2. \quad (38)$$

Only splittings with $z(1-z) > c_z k_{\text{T}}^2 / Q^2$ allow the variable $\lambda(y)$ in Eq. (A2) to be defined, so only these splittings are kinematically possible. We have set $a_{\perp}(z, k_{\text{T}}^2) = 1$ in the case that k_{T}^2 is too large to allow a splitting with momentum fraction z .

We can use the function $a_{\perp}(z, k_{\text{T}}^2)$ to define the unresolved region specified by the singular operator $\mathcal{D}^{[1,0]}$ for k_{T} ordering. We first address an issue concerning the

We will make use of this decomposition in this paper to treat the two terms differently.

V. UNRESOLVED REGION WITH ONE SCALE

We now consider the unresolved region for a splitting in a first order shower in the standard case that there is a single shower scale μ_{s} .

The operator $\mathcal{D}^{[1,0]}(\mu_{\text{s}})$ contains an integration over splitting variables (y, z, ϕ) with (y, z) integrated over the unresolved region defined by the scale μ_{s} . The shower splitting operator is given by the first order version of Eq. (12),

$$\mathcal{S}^{[1,0]}(\mu_{\text{s}}) = \frac{d}{d\mu_{\text{s}}} \mathcal{D}^{[1,0]}(\mu_{\text{s}}). \quad (34)$$

Integrating between a scale $\mu_{\text{s},1}$ and a slightly smaller scale $\mu_{\text{s},2}$ gives the exponent in Eq. (15) for shower evolution between these two scales,

$$\int_{\mu_{\text{s},2}}^{\mu_{\text{s},1}} d\mu_{\text{s}} \mathcal{S}^{[1,0]}(\mu_{\text{s}}) = \mathcal{D}^{[1,0]}(\mu_{\text{s},1}) - \mathcal{D}^{[1,0]}(\mu_{\text{s},2}). \quad (35)$$

Thus we integrate over the unresolved region for the larger scale omitting the unresolved region for the smaller scale.

There are several possibilities for how the unresolved region depends on the scale. In each of three cases that we consider, we adopt a different name for the shower scale, $\mu_{\text{s}}^2 = \mu_{\perp}^2$, $\mu_{\text{s}}^2 = \mu_{\Lambda}^2$, and $\mu_{\text{s}}^2 = \mu_{\text{Z}}^2$.

One possibility is to define the unresolved region for a splitting by $k_{\text{T}}^2 < \mu_{\perp}^2$, where k_{T}^2 was defined in Eq. (27). The angle variable ϑ is related to k_{T}^2 and z in any kinematically allowed splitting by

$$\vartheta = a_{\perp}(z, k_{\text{T}}^2), \quad (36)$$

where

range of k_{T}^2 . The argument of α_{s} used in DEDUCTOR and other shower generators is an approximation to k_{T}^2 .⁴ We cannot trust perturbation theory if α_{s} is not small. For this reason, a splitting with squared transverse momentum k_{T}^2 must be considered unresolved if k_{T}^2 is smaller than a value m_{\perp}^2 of order 1 GeV². The parameter m_{\perp}^2

⁴ Precisely, DEDUCTOR uses $k_{\text{T}}^2/z = (1-z)2\hat{p}_l \cdot \hat{p}_{m+1}$ in α_{s} . This is the same as k_{T}^2 for $(1-z) \rightarrow 0$. The splitting functions have no $z \rightarrow 0$ singularity.

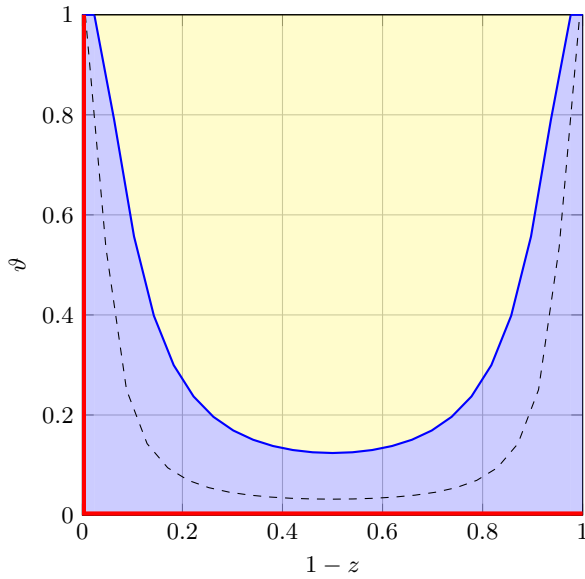


FIG. 4. Resolved and unresolved regions for fixed μ_{\perp}^2 . Here $a_{\perp} = 2$, $m_{\perp}^2 = 0.0005 Q^2$, and $\mu_{\perp}^2 = 0.002 Q^2$. (Thus m_{\perp}^2 is too small to play a role in this figure. The curve for m_{\perp}^2 is shown as a dashed line.)

is not an adjustable scale parameter but rather serves as a fixed cutoff parameter. We therefore define the unresolved region corresponding to a shower scale $\mu_s^2 \equiv \mu_{\perp}^2$ by

$$\vartheta < \max[a_{\perp}(z, \mu_{\perp}^2), a_{\perp}(z, m_{\perp}^2)]. \quad (39)$$

This is illustrated in Fig. 4 for the choice of shower scale parameter $\mu_{\perp}^2 = 0.002 Q^2$ with $a_{\perp} = 2$ and $m_{\perp}^2 = 0.0005 Q^2$. The singular surface, consisting of the lines $\vartheta = 0$ and $(1-z) = 0$ is indicated in red. The curve $\vartheta = a_{\perp}(z, \mu_{\perp}^2)$ with $\mu_{\perp}^2 = 0.002 Q^2$ is indicated in blue. The unresolved region is the blue region below this curve. Note that the unresolved region includes the entire singular surface. The resolved region is the yellow region above this curve.

If we use a k_T -ordered shower, then shower evolution from scale $\mu_{\perp,1}^2$ to a smaller scale $\mu_{\perp,2}^2$ includes splittings in the unresolved region for the larger scale but not splittings that are unresolved at the smaller scale, as in Eq. (35). This is illustrated in Fig. 5 for the case $\mu_{\perp,1}^2 = 0.004 Q^2$, $\mu_{\perp,2}^2 = 0.002 Q^2$. The region covered is displayed in green in the figure.

The unresolved region can also be defined by $\Lambda^2 < \mu_{\Lambda}^2$, supplemented by a fixed cut $k_T^2 < m_{\perp}^2$. Here Λ^2 is the virtuality variable defined in Eq. (25). The angle variable ϑ is related to $y = \Lambda^2/Q^2$ and z by

$$\vartheta = a_{\Lambda}(z, \Lambda^2), \quad (40)$$

where

$$a_{\Lambda}(z, yQ^2) = \frac{a_{\perp}y}{(1+y)^2z(1-z) + a_{\perp}y(1-4z(1-z))}. \quad (41)$$

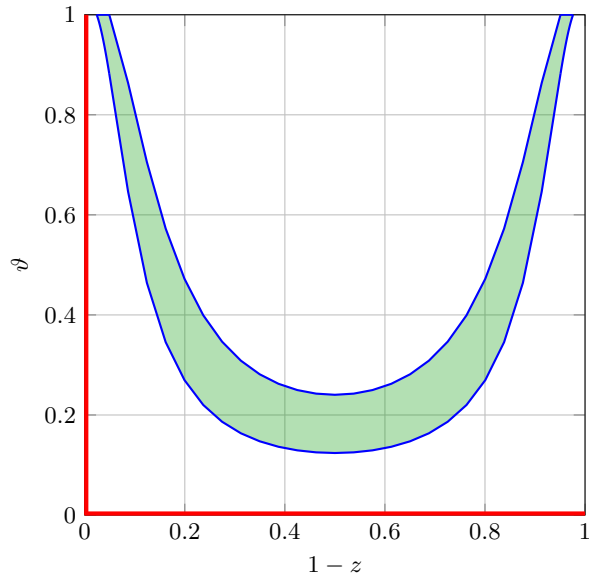


FIG. 5. Evolution in μ_{\perp}^2 for $0.002 < \mu_{\perp}^2/Q^2 < 0.004$. Here $a_{\perp} = 2$, $m_{\perp}^2 = 0.0005 Q^2$.

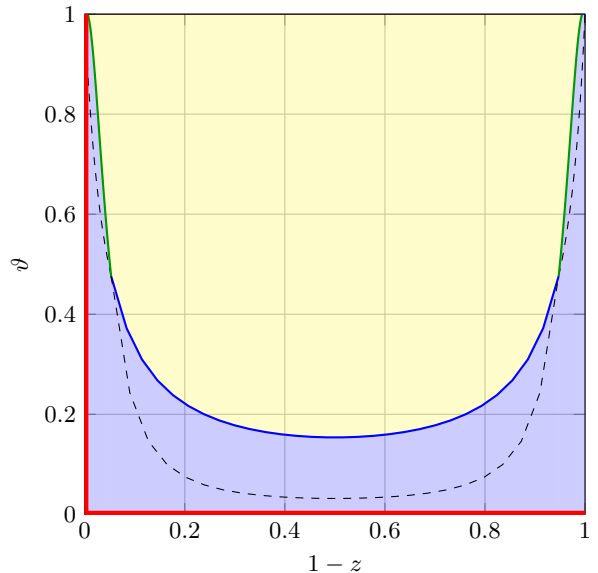


FIG. 6. Unresolved regions for fixed $\mu_{\Lambda}^2 = 0.02 Q^2$. Here $a_{\perp} = 2$ and $m_{\perp}^2 = 0.0005 Q^2$.

We can use the function $a_{\Lambda}(z, \Lambda^2)$ to define the unresolved region specified by the singular operator $\mathcal{D}^{(1,0)}$ for Λ ordering, which is the default choice in DEDUCTOR. Since DEDUCTOR uses an approximation to k_T^2 as the argument of α_s , we again do not allow k_T^2 to be smaller than a fixed cutoff parameter m_{\perp}^2 of order 1 GeV² in the resolved region. With this definition, the unresolved region for a given choice of the shower scale $\mu_s^2 \equiv \mu_{\Lambda}^2$ is

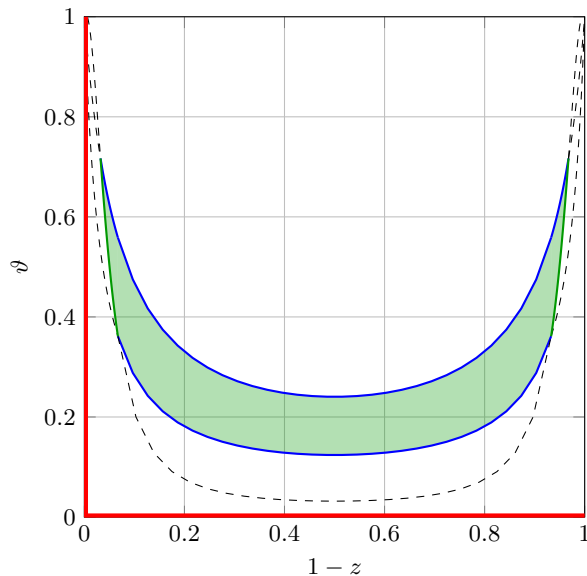


FIG. 7. Evolution in μ_Λ^2 with $m_\perp^2 = 0.0005 Q^2$. Here $a_l = 2$ and $0.016 < \mu_\Lambda^2/Q^2 < 0.032$. This figure is analogous to Fig. 5 for k_T ordering.

defined by⁵

$$\vartheta < \max[a_\Lambda(z, \mu_\Lambda^2), a_\perp(z, m_\perp^2)]. \quad (42)$$

This region is illustrated in Fig. 6 in the case $a_l = 2$ with $m_\perp^2 = 0.0005 Q^2$ for the choice of shower scale parameter $\mu_\Lambda^2 = 0.02 Q^2$. Again, the singular surface is indicated in red and the unresolved region is depicted in blue.

If we use a Λ -ordered shower with a k_T^2 cutoff at a small fixed scale $m_\perp^2 = 0.0005 Q^2$, then shower evolution from scale $\mu_{\Lambda,1}^2$ to a smaller scale $\mu_{\Lambda,2}^2$ includes splittings in the unresolved region for the larger scale but not splittings that are unresolved at the smaller scale. This is illustrated in Fig. 7 for the case $\mu_{\Lambda,1}^2 = 0.032 Q^2$, $\mu_{\Lambda,2}^2 = 0.016 Q^2$. The region covered is displayed in green in the figure. Note how the region of small $z(1-z)$ is removed by the m_\perp^2 cut.

Finally, we can use angular ordering and define the unresolved region by $\vartheta Q^2 < \mu_Z^2$, supplemented by a fixed cut $k_T^2 < m_\perp^2$. We define

$$a_Z(z, \vartheta Q^2) = \vartheta. \quad (43)$$

With this definition, the unresolved region for a given choice of the shower scale $\mu_s^2 \equiv \mu_Z^2$ is defined by

$$\vartheta < \max[a_Z(z, \mu_Z^2), a_\perp(z, m_\perp^2)]. \quad (44)$$

This region is illustrated in Fig. 8 in the case $a_l = 2$ with $m_\perp^2 = 0.0005 Q^2$ for the choice of shower scale parameter

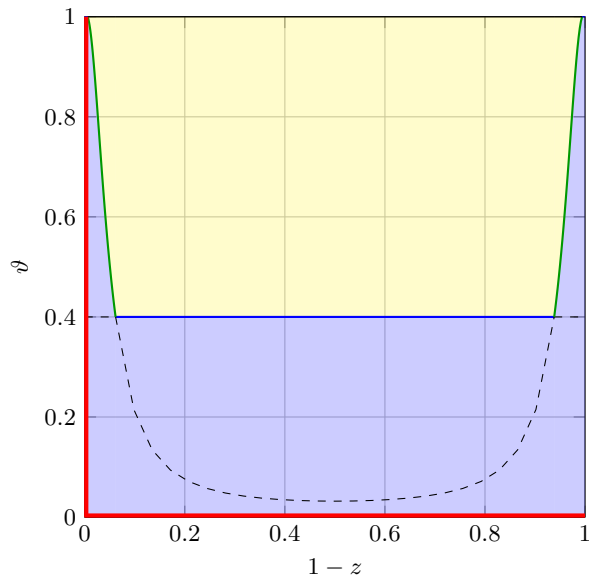


FIG. 8. Unresolved regions for fixed μ_Z^2 with cutoff $m_\perp^2 = 0.0005 Q^2$. Here $a_l = 2$ and $\mu_Z^2 = 0.4 Q^2$.

$\mu_Z^2 = 0.4 Q^2$. Again, the singular surface is indicated in red and the unresolved region is depicted in blue.

There is an important difference between the unresolved regions for Λ ordering, Fig. 6, and angular ordering, Fig. 8. With Λ ordering, we could set $m_\perp^2 = 0$. There would be a problem with α_s with an argument proportional to $(1-z)$ when $(1-z) \ll 1$, but this problem could be eliminated by letting the argument of α_s be yQ^2 . With angular ordering, if m_\perp^2 were zero, there would be a naked singularity: points $((1-z), \vartheta)$ with $(1-z) = 0$ are in the resolved region when $\vartheta > \mu_Z^2/Q^2$. Thus we need a nonzero m_\perp^2 with angular ordering.

We have described the unresolved region for three choices of a single ordering variable. Angular ordering is available in HERWIG [2, 19]. Variants of k_T ordering are used in PYTHIA [3], SHERPA [4], and DIRE [5]. The default ordering variable in DEDUCTOR [10] is Λ . The papers [20, 21] have a family of ordering choices defined by a parameter β . With $\beta = 0$, the ordering variable is a transverse momentum variable, although other features of the shower are not the same as in the DEDUCTOR shower. With $\beta = 1/2$, the ordering variable is not among those investigated in this paper but is roughly half way between k_T and Λ .

We note that the shower that we discuss here is a full dipole shower with interference between emitting a gluon from one parton and emitting the same gluon from a second parton. All that we do with angular ordering is to use the emission angle as the ordering variable. Thus no approximation involving averaging over the azimuthal angle of the emission is involved, as it is in HERWIG [2, 19].

⁵ If $\mu_\Lambda^2/Q^2 > (\sqrt{a_l} + \sqrt{a_l - 1})^{-2}$, then $a_\Lambda(z, \mu_\Lambda^2) > 1$ for $0 < z < 1$, so all splittings with $0 < \vartheta < 1$, $0 < z < 1$ are unresolved.

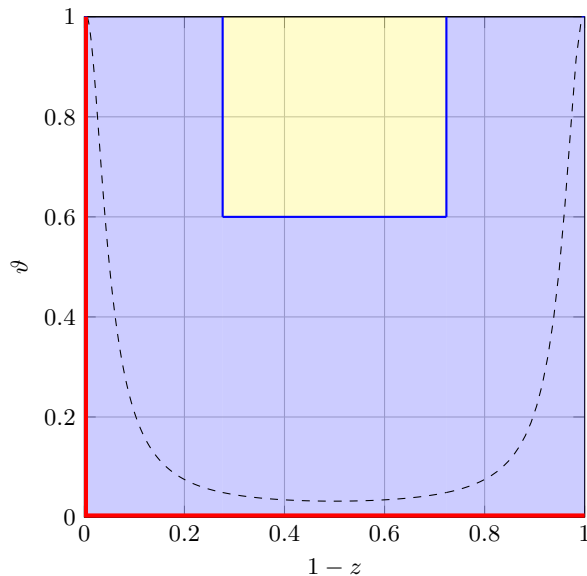


FIG. 9. Unresolved regions for fixed $\vec{\mu} = (\mu_E, \mu_\perp)$ with cutoff $m_\perp^2 = 0.0005 Q^2$. Here $a_l = 2$. The two scales are $\mu_E^2 = 0.2 Q^2$ and $\mu_\perp^2 = 0.6 Q^2$.

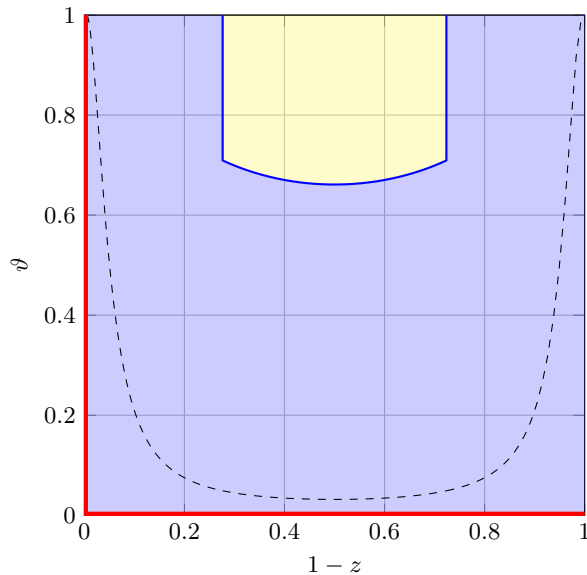


FIG. 10. Unresolved regions for fixed $\vec{\mu} = (\mu_E, \mu_\Lambda)$ with cutoff $m_\perp^2 = 0.0005 Q^2$ and $a_l = 2$. The two scales are $\mu_E^2 = 0.2 Q^2$ and $\mu_\Lambda^2 = 0.1 Q^2$.

VI. UNRESOLVED REGION WITH TWO SCALES

We now consider the unresolved region for a splitting when we use two independent scale parameters. Throughout this section, we also incorporate the fixed infrared cutoff $k_\perp^2 > m_\perp^2$.

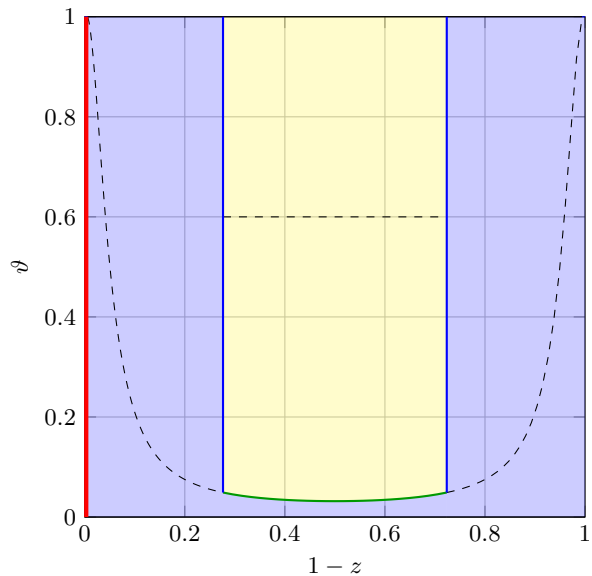


FIG. 11. Unresolved regions for fixed $\vec{\mu} = (\mu_E, \mu_\perp)$ with cutoff $m_\perp^2 = 0.0005 Q^2$ for $\mathcal{D}_{\text{soft}}^{(1)}(\vec{\mu})$. As in Fig. 9, we take $a_l = 2$, $\mu_E^2 = 0.2 Q^2$ and $\mu_\perp^2 = 0.6 Q^2$. For $\mathcal{D}_{\text{soft}}^{(1)}(\vec{\mu})$, the unresolved region is independent of μ_\perp^2 .

We let one scale be a collinear sensitive scale μ_C , which could be any of μ_\perp , μ_Λ , or μ_\perp . The scale μ_C controls at least the collinear singularity for one parton splitting into two. With $\mu_C = \mu_\perp$, this scale controls *only* the collinear singularity. The other singularity is the wide angle soft singularity, which is reached when a parton emits a gluon at a finite angle when the energy of the gluon approaches zero. We need a scale μ_E to control this singularity. The emitted gluon energy is proportional to $(1-z)$, so it is convenient to define an unresolved region parameterized by μ_E^2 by using an energy variable $4z(1-z)Q^2$. The factor z here is not important since there is no $z \rightarrow 0$ singularity in the splitting functions as defined in DEDUCTOR, but it is helpful to keep the scale definitions symmetric under $(1-z) \leftrightarrow z$. We define a function

$$a_E(z, \mu_E^2) = \begin{cases} 1 & \text{for } 4z(1-z)Q^2 < \mu_E^2 \\ 0 & \text{otherwise} \end{cases}. \quad (45)$$

We can use this function and our previously defined function $a_C(z, \mu_C^2)$ for $C = \perp, \Lambda$, or \perp to define an unresolved region for a given choice of two shower scales $\vec{\mu} = (\mu_E, \mu_C)$. We define the unresolved region by

$$\vartheta < \max[a_E(z, \mu_E^2), a_C(z, \mu_C^2), a_\perp(z, m_\perp^2)]. \quad (46)$$

This region is illustrated in Fig. 9 in the case $C = \perp$, $a_l = 2$ with $m_\perp^2 = 0.0005 Q^2$ for the choice of shower scales $\mu_E^2 = 0.2 Q^2$, $\mu_\perp^2 = 0.6 Q^2$. Again, the singular surface is indicated in red and the unresolved region is depicted in blue. A point $(1-z, \vartheta)$ is in the unresolved region if $4z(1-z) < \mu_E^2/Q^2$ or $\vartheta < \mu_\perp^2/Q^2$. The point is

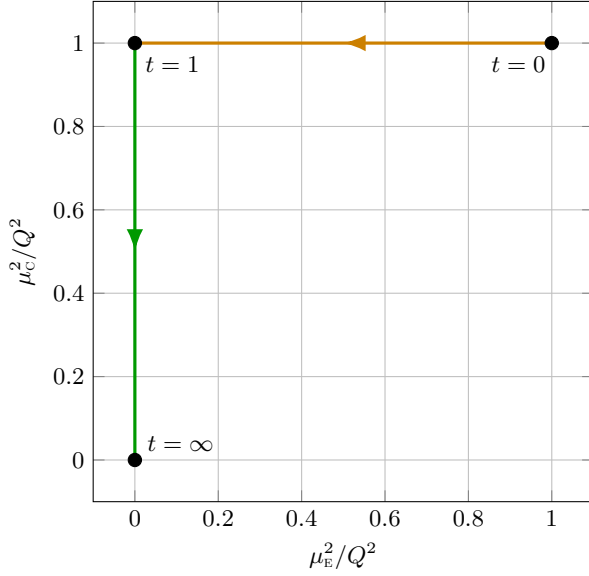


FIG. 12. Evolution path with two segments.

also in the unresolved region if $k_T^2 < m_\perp^2$, although this cutoff does not play a role in Fig. 9.

The unresolved region specified by Eq. (46) is illustrated in Fig. 10 for the case $C = \Lambda$, with $\mu_E^2 = 0.2 Q^2$, $\mu_\Lambda^2 = 0.1 Q^2$.

As foreseen in Eq. (33), we can divide $\mathcal{D}^{[1,0]}(\vec{\mu})$ into a part $\mathcal{D}_{\text{sc}}^{[1,0]}(\vec{\mu})$ with both soft and collinear singularities and a part $\mathcal{D}_{\text{soft}}^{[1,0]}(\vec{\mu})$ with only soft singularities. Since $\mathcal{D}_{\text{soft}}^{[1,0]}(\vec{\mu})$ lacks the collinear singularity, we can treat it differently. We define the unresolved region for $\mathcal{D}_{\text{soft}}^{[1,0]}(\vec{\mu})$ by

$$\vartheta < \max[a_E(z, \mu_E^2), a_\perp(z, m_\perp^2)]. \quad (47)$$

That is, we replace μ_c^2 by zero for $\mathcal{D}_{\text{soft}}^{[1,0]}(\vec{\mu})$. This resulting unresolved region for $\mathcal{D}_{\text{soft}}^{[1,0]}(\vec{\mu})$ for $C = \angle$ is illustrated in Fig. 11. No lower limit for ϑ is needed for $\mathcal{D}_{\text{soft}}^{[1,0]}(\vec{\mu})$ since it has no $\vartheta \rightarrow 0$ singularity. The only cutoff that applies for small ϑ is $k_T^2 > m_\perp^2$.

Now, to define the shower operator $\mathcal{U}(t_f, 0)$, we need to define initial and final scales $\vec{\mu}(0) = \vec{\mu}_H$ and $\vec{\mu}(t_f) = \vec{\mu}_f$ and a path $\vec{\mu}(t)$ that connects them. For the hard scales we take $\mu_{c,H}^2 = Q^2$ and $\mu_{e,H}^2 = Q^2$. For the infrared limiting values $\vec{\mu}_f$, we could take values on the order of $\mu_{c,f}^2 = \mu_{e,f}^2 = 1 \text{ GeV}^2$. However, there is already a cutoff $k_T^2 > m_\perp^2$, so it suffices to set $\mu_{c,f}^2 = \mu_{e,f}^2 = 0$.

Next, we need a path, $\vec{\mu}(t)$. We choose a path with two segments, illustrated in Fig. 12. In the first segment, for $0 < t < 1$, we choose $\mu_c^2 = Q^2$ and $\mu_e^2 = (1-t)Q^2$. On this segment of the path, the corner of the rectangle in Fig. 9 is defined by $4z(1-z)$ decreasing from 1 to 0 and ϑ fixed at 1. In the second part, for $1 < t < t_f = \infty$, we choose $\mu_c^2 = e^{-(t-1)}Q^2$ and $\mu_e^2 = 0$. On this segment of

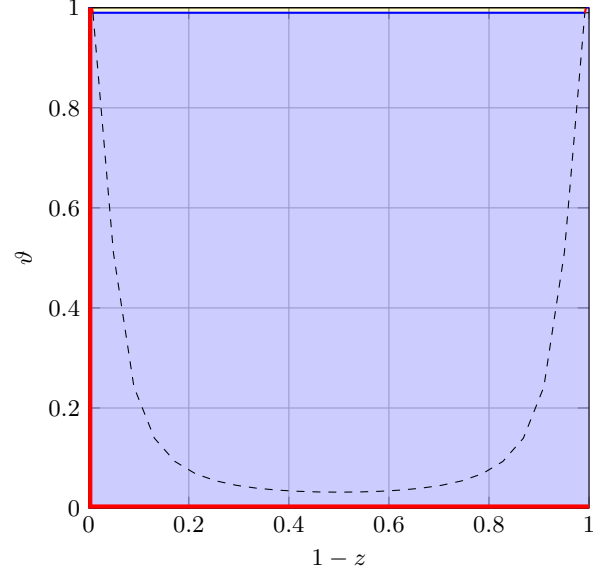


FIG. 13. Unresolved region for $\mathcal{D}_{\text{sc}}^{[1,0]}(\vec{\mu})$ at the end of the first stage of evolution. Here $a_l = 2$ and $m_\perp^2 = 0.0005 Q^2$.

the path, the corner of the rectangle in Fig. 9 is defined by $4z(1-z)$ fixed at 0 and ϑ decreasing from 1 to 0. Thus the path is

$$\begin{aligned} \vec{\mu}(t) &= \begin{bmatrix} \mu_E(t) \\ \mu_C(t) \end{bmatrix} \\ &= \theta(0 < t < 1) \sqrt{Q^2} \begin{bmatrix} \sqrt{1-t} \\ 1 \end{bmatrix} \\ &\quad + \theta(t > 1) \sqrt{Q^2} \begin{bmatrix} 0 \\ e^{(1-t)/2} \end{bmatrix}. \end{aligned} \quad (48)$$

The unresolved region for $\mathcal{D}_{\text{sc}}^{[1,0]}(\vec{\mu})$ at the end of first segment of the path is shown in Fig. 13. The same figure applies for any of our choices for C because $a_c(z, Q^2) \geq 1$ for $C = \perp, \Lambda$, or \angle . There is no change in $\mathcal{D}_{\text{sc}}^{[1,0]}(\vec{\mu})$ in this segment. Everything remains unresolved. The unresolved region for $\mathcal{D}_{\text{soft}}^{[1,0]}(\vec{\mu})$ at the end of first segment of the path is shown in Fig. 14. In this segment, $\mathcal{D}_{\text{soft}}^{[1,0]}(\vec{\mu})$ changes substantially, so that at the end of this segment of the path, the unresolved region is only the region with $k_T^2 < m_\perp^2$.

In the second segment of the path, the unresolved region for $\mathcal{D}_{\text{soft}}^{[1,0]}(\vec{\mu})$ does not change at all. It remains as depicted in Fig. 14. In this second segment, $\mathcal{D}_{\text{sc}}^{[1,0]}(\vec{\mu})$ changes substantially, so that at the end of this segment of the path, the unresolved region is only the region with $k_T^2 < m_\perp^2$. This is the region that was already depicted in Fig. 14, but now it applies to $\mathcal{D}_{\text{sc}}^{[1,0]}(\vec{\mu})$.

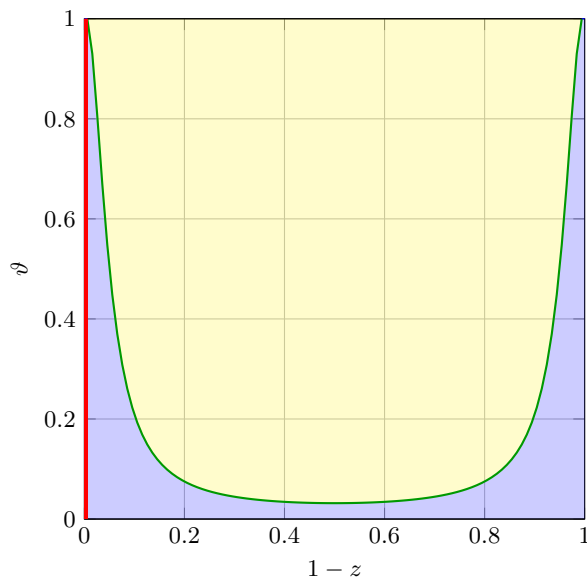


FIG. 14. Unresolved region for $\mathcal{D}_{\text{soft}}^{[1,0]}(\vec{\mu})$ at the end of the first stage of evolution. Here $a_l = 2$ and $m_{\perp}^2 = 0.0005 Q^2$.

VII. EVOLUTION WITH TWO SCALES

The singular operator $\mathcal{D}(\vec{\mu})$ has a perturbative expansion (19). The shower generator $\mathcal{S}_j(\vec{\mu})$ is defined in Eq. (12). The index $j \in \{E, C\}$ includes two scale choices. The shower generator has a perturbative expansion

$$\mathcal{S}_j(\vec{\mu}) = \frac{\alpha_s}{2\pi} \mathcal{S}_j^{(1)}(\vec{\mu}) + \mathcal{O}(\alpha_s^2). \quad (49)$$

From Eq. (12), the first order contribution is

$$\mathcal{S}_j^{(1)}(\vec{\mu}) = \frac{\partial}{\partial \mu_j} \mathcal{D}^{(1)}(\vec{\mu}). \quad (50)$$

In a first order shower, we truncate the expansion of $\mathcal{S}_j(\vec{\mu})$ at first order,

$$\mathcal{S}_j(\vec{\mu}) = \frac{\alpha_s}{2\pi} \mathcal{S}_j^{(1)}(\vec{\mu}). \quad (51)$$

To obtain the shower evolution operator $\mathcal{U}(t_2, t_1)$ following the chosen path $\vec{\mu}(t)$, we solve the differential equation Eq. (13). In general, this gives us the group multiplication property

$$\mathcal{U}(t_2, t_1) = \mathcal{U}(t_2, \tau) \mathcal{U}(\tau, t_1). \quad (52)$$

Our path has two segments, $0 < t < 1$ and $1 < t < \infty$. This gives

$$\mathcal{U}(\infty, 0) = \mathcal{U}(\infty, 1) \mathcal{U}(1, 0). \quad (53)$$

We have divided $\mathcal{D}^{(1)}(\vec{\mu})$ into a part $\mathcal{D}_{\text{sc}}^{(1)}(\vec{\mu})$ with both soft and collinear singularities and a part $\mathcal{D}_{\text{soft}}^{(1)}(\vec{\mu})$ with only soft singularities, as in Eq. (33). We recall that

only μ_E changes on the first segment of the path and this change affects only $\mathcal{D}_{\text{soft}}^{(1)}(\vec{\mu})$. We also recall that only μ_C changes on the second segment of the path and this change affects only $\mathcal{D}_{\text{sc}}^{(1)}(\vec{\mu})$. Then

$$\mathcal{U}(1, 0) = \mathbb{T} \exp \left\{ - \int_0^1 dt \frac{d\mu_E(t)}{dt} \mathcal{S}_E^{\text{soft}}(\vec{\mu}(t)) \right\} \quad (54)$$

and

$$\mathcal{U}(\infty, 1) = \mathbb{T} \exp \left\{ - \int_1^\infty dt \frac{d\mu_C(t)}{dt} \mathcal{S}_C^{\text{sc}}(\vec{\mu}(t)) \right\}. \quad (55)$$

In this formulation the parton shower, the result depends on what we choose for $\mathcal{D}_{\text{soft}}^{(1)}(\vec{\mu})$ and $\mathcal{D}_{\text{sc}}^{(1)}(\vec{\mu})$. We can choose $\mathcal{D}_{\text{soft}}^{(1)}(\vec{\mu}) = 0$. Then $\mathcal{D}_{\text{sc}}^{(1)}(\vec{\mu})$ is all of $\mathcal{D}^{(1)}(\vec{\mu})$. When $\mu_C = \mu_{\angle}$ this gives us a simple angular ordered shower, as in Eq. (44) and Fig. 8. The only difference is conceptual. First, $\mathcal{D}_{\text{sc}}^{(1)}(\vec{\mu})$ and its inverse $[\mathcal{D}_{\text{sc}}^{(1)}(\vec{\mu})]^{-1}$ are well defined at the hard scale. This is important because $[\mathcal{D}_{\text{sc}}^{(1)}(\vec{\mu})]^{-1}$ plays the role of removing infrared singularities from the hard scattering cross section calculated at next-to-leading order [1]. Second, with the two scale formulation, we could have eliminated the m_{\perp}^2 cut. Then it would have been natural to choose a nonzero endpoint $\mu_{E,f}^2 \sim 1 \text{ GeV}^2$ for the evolution in μ_E in the first segment of the path. This would leave us with no naked singularity in a natural way.

There are a number of nonzero choices we could make for $\mathcal{D}_{\text{soft}}^{(1)}(\vec{\mu})$, letting $\mathcal{D}_{\text{sc}}^{(1)}(\vec{\mu}) = \mathcal{D}^{(1)}(\vec{\mu}) - \mathcal{D}_{\text{soft}}^{(1)}(\vec{\mu})$. One possibility is to define $\mathcal{D}_{\text{sc}}^{(1)}(\vec{\mu})$ so that, although it has a soft \times collinear double singularity, it has only a minimal wide-angle soft singularity. Whatever choice we make, the evolution $\mathcal{U}(1, 0)$, using $\mathcal{D}_{\text{soft}}^{(1)}(\vec{\mu})$, comes first, followed by evolution $\mathcal{U}(\infty, 1)$, using $\mathcal{D}_{\text{sc}}^{(1)}(\vec{\mu})$ with an ordering prescription such as angular ordering, Λ ordering, or k_T ordering.

This two scale formulation of a parton shower is reminiscent of soft-collinear effective theory (SCET). Suppose that we want to measure an observable that is nonzero when there are at least N hard jets. We start with a hard scattering that produces N hard jets. With a cut on $(N-1)$ jettiness [22], $\tau_{N-1} > \tau_{\text{min}}$, we ensure that the hard partons constitute N jets and not $N-1$ jets. With this as the hard state, the operator $\mathcal{S}_E^{\text{soft}}(\vec{\mu}(t))$ in $\mathcal{U}(1, 0)$ produces soft wide-angle radiation from the N hard jets, analogously to the soft factor in SCET. In the second segment of the shower evolution, $\mathcal{U}(\infty, 1)$ can add more soft radiation. However, if $\mathcal{S}_C^{\text{sc}}(\vec{\mu}(t))$ (where $C = \angle, \Lambda, \perp$ or some other choice) is defined to have only minimal wide-angle soft singularities, it is the first segment, involving $\mathcal{S}_E^{\text{soft}}(\vec{\mu}(t))$ that will dominate the soft radiation between the jets. Then the second evolution segment acts as the collinear factor in a SCET analysis and fills in the collinear radiation for each jet.

VIII. IMPROVED COLOR WITH TWO SCALES

In this section, we describe how one might use the choices available when using the two scales, μ_C and μ_E , to improve the treatment of color in the shower in a practical way.

First, we provide some background on color in parton showers. The most widely used parton shower event generators [2–4] use the leading color (LC) approximation, which captures just the leading term in an expansion in powers of $1/N_c^2$, where $N_c = 3$ is the number of colors. Here one simply supplies a color factor $C_F = (N_c^2 - 1)/(2N_c)$ or $C_A = N_c$ for emission of a gluon from a quark or gluon line, respectively, or else a factor $T_R = 1/2$ for a gluon splitting to $q + \bar{q}$. To go beyond the LC approximation one needs to treat the color carried by quarks and gluons as fully quantum mechanical variables.

Throughout this paper, we have described color as fully quantum mechanical using a vector space for parton color with basis vectors $|\{c, c'\}_m\rangle$ [6]. The basis vector $|\{c, c'\}_m\rangle$ represents a color density matrix $|\{c\}_m\rangle\langle\{c'\}_m|$, where $|\{c\}_m\rangle$ is a basis vector for the space of quantum color states for m partons. (DEDUCTOR uses the trace basis, but other choices are possible.) This description, with a somewhat different notation, is used in the recent papers [23–29] to study color in parton shower evolution, accounting approximately for both real emission graphs and virtual exchange graphs. Other papers have used the color density matrix, but for the description of just real emissions [30–32]. Ref. [21] has worked to improve the treatment of color in parton showers without tying the description to the color density matrix.

One can express the evolution equations for a first order dipole shower so that it evolves with full color [6]. However, some approximation is needed for a shower realized in computer code. The DEDUCTOR shower uses what we call the LC+ approximation⁶ for color [9]. This is an improvement over the LC approximation. The splitting operators with this approximation, $\mathcal{S}_j^{\text{LC+}}(\vec{\mu})$, are, however, still approximate in color, leaving a difference

$$\Delta\mathcal{S}_j(\vec{\mu}) = \mathcal{S}_j(\vec{\mu}) - \mathcal{S}_j^{\text{LC+}}(\vec{\mu}). \quad (56)$$

Simply using $\mathcal{S}_j^{\text{LC+}}$ would give us an uncontrolled approximation since we would not know the size of corrections from $\Delta\mathcal{S}_j(\vec{\mu})$. DEDUCTOR allows a systematically improvable approximation: the user can compute corrections proportional to powers $[\Delta\mathcal{S}_j]^N$ of $\Delta\mathcal{S}_j$ (with a single scale μ_s) [14–16]. Any power N is allowed. However, including powers of $\Delta\mathcal{S}_j$ is computationally complicated and makes the program run more slowly. This leads to practical limits to the size of N .

It would certainly be desirable to have particular choice of $\mathcal{S}_E^{\text{soft}}(\vec{\mu}(t))$ that results in making the inclusion of $\Delta\mathcal{S}_j(\vec{\mu})$ computationally simpler. With this in mind, we note that the LC+ approximation has an important property. At each splitting, the leading soft \times collinear singularity and the leading collinear singularity are treated exactly with respect to color [9]. That is, $\Delta\mathcal{S}_j(\vec{\mu})$ has no collinear singularity. Thus we can set

$$\begin{aligned} \mathcal{S}_j^{\text{sc}}(\vec{\mu}(t)) &= \mathcal{S}_j^{\text{LC+}}(\vec{\mu}(t)), \\ \mathcal{S}_j^{\text{soft}}(\vec{\mu}(t)) &= \Delta\mathcal{S}_j(\vec{\mu}(t)). \end{aligned} \quad (57)$$

With this choice, $\mathcal{U}(\infty, 1)$ in Eq. (53) is exact in color and the corrections to the LC+ approximation appear in the factor $\mathcal{U}(1, 0)$. This is significant for two reasons. First, the corrections to the LC+ approximation appear in one place, rather than appearing throughout the shower, interleaved with LC+ splittings, as in Refs. [14–16]. Second, the factor $\mathcal{U}(1, 0)$ operates on the hard scattering state with which the shower begins. This state is simple because it has few partons.

For $\mathcal{U}(1, 0)$, we can expand Eq. (54) in powers of $\Delta\mathcal{S}$,

$$\begin{aligned} \mathcal{U}(1, 0) &= 1 - \int_0^1 dt \frac{d\mu_E(t)}{dt} \Delta\mathcal{S}_E(\vec{\mu}(t)) \\ &+ \int_0^1 dt_2 \frac{d\mu_E(t_2)}{dt_2} \int_0^{t_2} dt_1 \frac{d\mu_E(t_1)}{dt_1} \\ &\quad \times \Delta\mathcal{S}_E(\vec{\mu}(t_2)) \Delta\mathcal{S}_E(\vec{\mu}(t_1)) \\ &+ \dots, \end{aligned} \quad (58)$$

keeping terms up to order $[\Delta\mathcal{S}_E]^N$, where N is chosen by the user. A more elaborate treatment is possible, but, given the simplicity of the hard scattering state to which $\mathcal{U}_c(1, 0)$ is applied, this very simple treatment should suffice.

If we start with the simplest process in e^+e^- annihilation, $e^+e^- \rightarrow q\bar{q}$, this is even simpler. Because the q and \bar{q} are each other's color connected partners, we have for the two parton $q\bar{q}$ state

$$\Delta\mathcal{S}_E(\vec{\mu}(t))|\{p, f, c, c'\}_2\rangle = 0. \quad (59)$$

Thus $\mathcal{U}(1, 0)|\{p, f, c, c'\}_2\rangle = |\{p, f, c, c'\}_2\rangle$, so

$$\mathcal{U}(\infty, 0)|\{p, f, c, c'\}_2\rangle = \mathcal{U}(\infty, 1)|\{p, f, c, c'\}_2\rangle. \quad (60)$$

We can write this in more detail. We choose the evolution scale in $\mathcal{U}(\infty, 1)$ as $\mu_c = \mu_\perp$, μ_Λ , or μ_\perp according to our preference and use $\mathcal{S}^{\text{LC+}}(\mu_c) = \mathcal{S}_C^{\text{LC+}}(\mu_E, \mu_c)$ with $\mu_E = 0$. Then

$$\begin{aligned} \mathcal{U}(\infty, 0)|\{p, f, c, c'\}_2\rangle &= \mathbb{T} \exp \left\{ \int_0^Q d\mu_c \mathcal{S}^{\text{LC+}}(\mu_c) \right\} \\ &\quad \times |\{p, f, c, c'\}_2\rangle. \end{aligned} \quad (61)$$

It is remarkable that the LC+ approximation for color gives the exact answer in this case. However, one should

⁶ The LC+ approximation is defined using the trace basis for color. There is no equivalent approximation in the color flow basis.

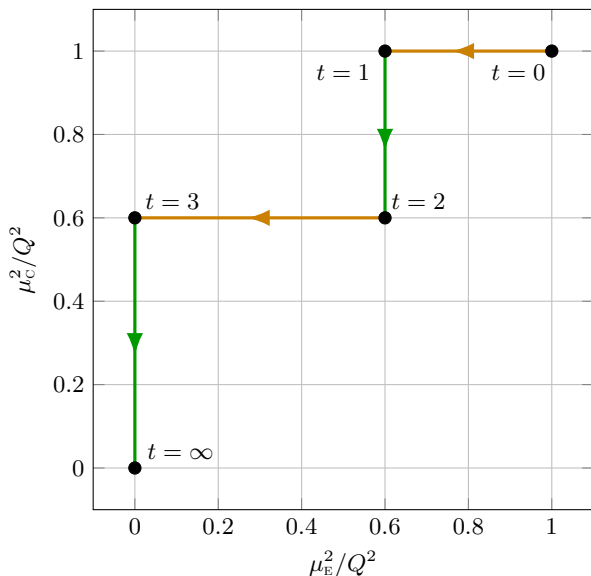


FIG. 15. Evolution path with four segments.

be careful about what “exact” means. A first order parton shower does not represent full QCD exactly. Two different choices for the choice of shower scale scheme will give two different parton shower algorithms. When we work within a framework that encompasses parton showers at any perturbative order [1], we see that the first of two algorithms can, in principle, be mapped into the second by adding order α_s^2 and higher order terms to the splitting functions of the second. With both splitting functions truncated at order α_s , the two algorithms give different results. The difference is a measure of the uncertainty inherent in using a first order shower.

Thus it is indeed remarkable that the LC+ approximation for color is exact in this case, but the meaning of this statement is that differences from the LC+ approximation in the one scale treatment can be absorbed into terms in the shower splitting functions that are higher order in α_s in the two scale treatment.

We emphasize that e^+e^- annihilation with $e^+e^- \rightarrow q\bar{q}$ as the hard process is a special case. A hard scattering process with m final state partons with $m > 2$ will lead to $\mathcal{U}(1,0)|\{p, f, c, c'\}_m$ being nontrivial. Then one will need to use Eq. (58) for $\mathcal{U}(1,0)$.

IX. MORE COMPLEX CONTOUR

One might argue that the two segment contour is too extreme since we put all the wide angle soft contributions just after the hard interaction. This might provide a good approximation if we consider a measurement that examines just the jets created by the initial hard partons, so that we wish to have the shower generate soft gluons that can see only the initial hard jets.

But what happens if our observable is sensitive to the structure of extra jets in addition to the initial hard jets. With the two-segment path, these jets are not corrected by any wide angle soft emissions beyond those generated within the LC+ approximation. We can adapt the evolution path for such an observable by using a four segment contour as illustrated in Fig. 15. This path can be parameterized similarly to Eq. (48).

On the first segment of the contour, the evolution operator is

$$\mathcal{U}(1,0) = \mathbb{T} \exp \left\{ - \int_0^1 dt \frac{d\mu_E(t)}{dt} \Delta \mathcal{S}_E(\vec{\mu}(t)) \right\}. \quad (62)$$

Only the wide angle soft operator $\Delta \mathcal{S}_E(\vec{\mu})$ contributes. This comes right after the hard stage and tries to add partons with rather large energy and large emission angle. Small angle radiation is suppressed in $\Delta \mathcal{S}_E(\vec{\mu})$ and small energy emissions are not allowed because μ_E^2 is never small on this path segment.

On the second segment of the contour, the evolution operator is

$$\mathcal{U}(2,1) = \mathbb{T} \exp \left\{ - \int_1^2 dt \frac{d\mu_C(t)}{dt} \mathcal{S}_C^{\text{LC}+}(\vec{\mu}(t)) \right\}. \quad (63)$$

We have evolution in μ_C^2 in the LC+ approximation for color, with a condition on the energy of the emitted parton, $4z(1-z)Q^2 > 0.6Q^2$ (in this example). Since μ_C^2 is never small on this path segment, the radiation produced is neither very soft nor very collinear. We expect jets from this segment that are resolvable from each other at a fairly large scale.

The evolution operator for the third part of the shower evolution is

$$\mathcal{U}(3,2) = \mathbb{T} \exp \left\{ - \int_2^3 dt \frac{d\mu_E(t)}{dt} \mathcal{S}_E(\vec{\mu}(t)) \right\}. \quad (64)$$

This is different than the evolution on the first segment. Here the whole splitting operator $\mathcal{S}_E(\vec{\mu}) = \mathcal{S}_E^{\text{LC}+}(\vec{\mu}) + \Delta \mathcal{S}_E(\vec{\mu})$ contributes to the soft evolution. It is still only wide angle soft effect. For emissions created by $\mathcal{S}_C^{\text{LC}+}$, the emission angle is bounded from below because $\mu_C^2 = 0.6$ (in this example). For emissions created by $\Delta \mathcal{S}_E(\vec{\mu})$, we do not have a direct lower bound on the emission angle, but the small angle emissions are suppressed by the splitting function. We expect that this part of the evolution could be treated perturbatively as in Eq. (58).

The evolution operator for the fourth part of the shower evolution is

$$\mathcal{U}(\infty,3) = \mathbb{T} \exp \left\{ - \int_3^\infty dt \frac{d\mu_C(t)}{dt} \mathcal{S}_C^{\text{LC}+}(\vec{\mu}(t)) \right\}. \quad (65)$$

This gives soft-collinear evolution using the LC+ approximation, just as in the two segment case. We expect the emissions from the smallest values of μ_C^2 on this segment to be unresolved by the observable considered.

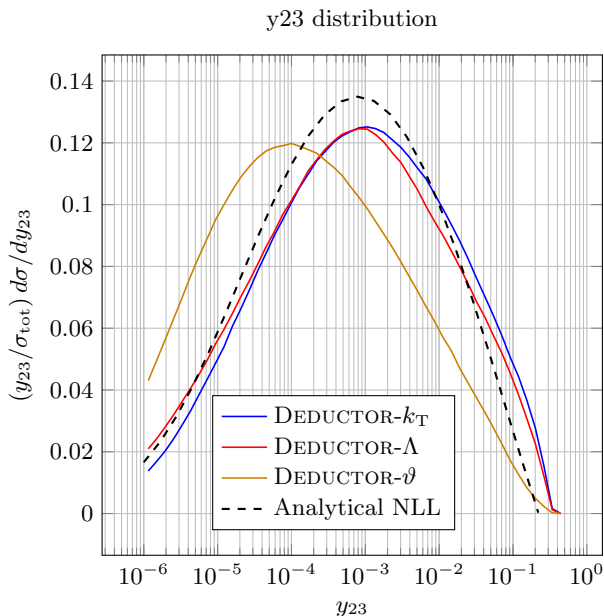


FIG. 16. The y_{23} distribution with the Cambridge algorithm.

X. COMPARISONS FOR e^+e^- ANNIHILATION AT 10 TEV

In this section, we study e^+e^- annihilation at $\sqrt{Q^2} = 10$ TeV, with the aims of demonstrating the practical application of the methods described in this paper, exploring the differences among the choices $\mu_C^2 = \mu_\perp^2$, μ_Λ^2 , and μ_ϑ^2 , and testing the dependence on the treatment color.

The hard scattering process is $e^+e^- \rightarrow q\bar{q}$, with more partons being provided by the parton shower. There are no data at such a large Q^2 , but with a large Q^2 , there is more room for shower evolution between the hard scale and the roughly 1 GeV scale at which we stop the shower. We use the DEDUCTOR parton shower to examine two jet production as a function of the resolution parameter y_{cut} using the Cambridge jet algorithm [33].

The fraction of events with exactly two jets is $(1/\sigma_{\text{tot}}) \sigma(2 \text{ jets}, y_{\text{cut}})$. For each event, there is a value y_{23} of the resolution parameter at which the event changes a two jet event to a three jet event. The distribution of $\log(y_{23})$ is

$$\frac{y_{23}}{\sigma_{\text{tot}}} \frac{d\sigma}{dy_{23}} = \left[\frac{y_{\text{cut}}}{\sigma_{\text{tot}}} \frac{d\sigma(2 \text{ jets}, y_{\text{cut}})}{dy_{\text{cut}}} \right]_{y_{\text{cut}}=y_{23}}. \quad (66)$$

We will study the behavior of this distribution.

We use a version⁷ of DEDUCTOR that is designed to include k_T ordering, Λ ordering, and angular ordering so

that only the ordering variable changes among the three choices.

We use the two segment scheme, Eq. (48) and Fig. 12, with three choices for the primary ordering scale, $\mu_C = \mu_\perp$ for k_T ordering, $\mu_C = \mu_\Lambda$ for Λ ordering, and $\mu_C = \mu_\vartheta$ for angular ordering. In each case, the primary evolution uses the LC+ approximation for color, so that the soft splitting operator is the difference, $\Delta S_j(\vec{\mu})$, between splitting with full color and splitting with the LC+ approximation for color, Eq. (57). Since we start with just a $q\bar{q}$ state and the LC+ approximation is exact for such a state, there is no evolution on the first segment of the path. For each choice of ordering scale, we let the m_\perp^2 cut end the shower. We choose $m_\perp^2 = 1 \text{ GeV}^2$. We do not provide a hadronization stage for the shower.

With the LC+ approximation in DEDUCTOR, the shower can generate contributions with values greater than zero of a parameter called the color suppression index, I [9]. These contributions are suppressed by a factor of at least $1/N_c^I$. The user can choose a value I_{max} such that values of I greater than I_{max} are not generated [14]. We choose $I_{\text{max}} = 4$.

The nominal renormalization scale according to the formulation given above for $\mathcal{S}_C^{\text{LC}+}(\vec{\mu})$ is $\mu_R = \mu_C$ or, more generally, some function of the scales $\vec{\mu}$, Eq. (5). However, DEDUCTOR attempts to incorporate some contributions from higher order splitting functions by evaluating α_s in the splitting functions at $\mu^2 = k_T^2/z = (1-z)2\hat{p}_\perp \cdot \hat{p}_{m+1}$.

In Fig. 16, we show the results for $(y_{23}/\sigma_{\text{tot}}) d\sigma/dy_{23}$ as a function of y_{23} for k_T ordering, Λ ordering, and angular (ϑ) ordering in the second segment of the two segment path in Fig. 12. We also show the next-to-leading-log (NLL) analytic expectation [34, 35] for this quantity. We see that the distribution for Λ ordering lies between the distributions for k_T ordering and for angular ordering. This was to be expected because, according to Eqs. (27) and (31), $k_T^2 < \Lambda^2 < \vartheta Q^2$ for any splitting. The results for k_T ordering and Λ ordering are close to each other and are quite close to the NLL analytic expectation. The angular ordering result is substantially different from the k_T ordering and Λ ordering results and the NLL analytic expectation. We do not have a satisfying explanation for this behavior, but we note that an analysis in Appendix B along the lines of Ref. [18] indicates that for the thrust, T , distribution, the angular ordered version of the algorithm fails to sum large logarithms of $1-T$ at the NLL or even LL level.

As discussed in Sec. VIII, because of the nature of the LC+ approximation and the simple nature of the $q\bar{q}$ hard state, the results in Fig. 16 are exact in color. That is, whatever is lacking in the color treatment would be corrected up to order α_s^3 if we had α_s^2 corrections to the shower splitting functions. It seems a reasonable conjecture that the color dependence of these α_s^2 corrections are numerically unimportant. To address this question, we can use the previous version (v. (3.0.3)) of DEDUCTOR, in which there is a single shower scale μ_s . The default

⁷ This version, DEDUCTOR v. 3.4.99, is available at <http://www.desy.de/~znagy/deductor/> and <http://pages.uoregon.edu/soper/deductor>.

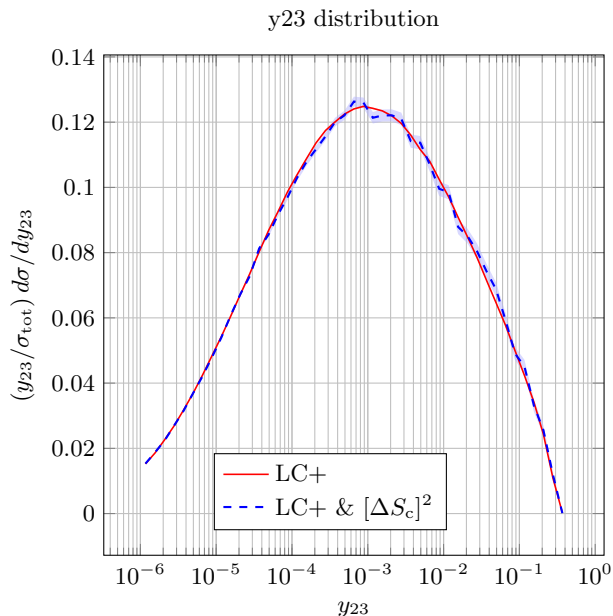


FIG. 17. The y_{23} distribution with the Cambridge algorithm using a calculation with just one scale μ_s . Results with just the LC+ approximation and with up to two units of the color correction operator ΔS_c are compared.

shower uses the LC+ approximation, but the user can add powers of ΔS_c perturbatively, interleaved with the LC+ evolution [14]. Our conjecture implies that the effect of adding ΔS_c powers is not numerically important in the present case of e^+e^- annihilation with a $q\bar{q}$ hard state.

To test this conjecture, we choose Λ ordering in DEDUCTOR-(3.0.3) and compare the result with the LC+ approximation with the result with up to two powers of ΔS_c added. The result is shown in Fig. 17. We see that adding ΔS_c powers makes the program run more slowly and thus increases the statistical errors. However, within the statistical errors (indicated by the band in Fig. 17), adding ΔS_c powers makes no difference to the result.

XI. SUMMARY AND OUTLOOK

In a parton shower, the state of many partons evolves as partons split with increasing “shower time” t . For a first order shower, one parton can split into two partons as dictated by three splitting variables such as (k_T, z, ϕ) . We have taken the view that for any t there is a resolvable region and an unresolvable region in the space of parton splitting variables. As t increases, more splittings become resolvable, so that there is a probability for a newly resolvable splitting to occur. The surface that divides the two regions can be parameterized by variables $\vec{\mu}$, with functions $\vec{\mu}(t)$ specifying the progression of boundary surfaces.

One could have any number of parameters μ_n to describe a surface in the space of parton splitting variables. Parton shower algorithms typically use one. In this paper, we use two parameters. We choose the first to be a parameter μ_E that provides a cut on the energy of an emitted parton. We choose the second parameter to be μ_C , which could be any of μ_\perp , μ_Λ , or μ_\angle . In single variable evolution, this would correspond, respectively, to k_T , Λ , or angular ordering, as described in Sec. V.

The probability for parton splitting in a first order shower is determined (using Eq. (A4)) by splitting operators \mathbf{D}_l , where l is the index of the parton that splits and where \mathbf{D}_l is an operator on the color space of the partons and a function of the parton momenta and flavors. These operators can be decomposed into two terms

$$\mathbf{D}_l = \mathbf{D}_l^{\text{sc}} + \mathbf{D}_l^{\text{soft}}, \quad (67)$$

where $\mathbf{D}_l^{\text{soft}}$ is singular for soft emissions but is not singular for collinear emissions (or for soft \times collinear emissions). We have adopted an especially useful way to do this by defining

$$\mathbf{D}_l^{\text{sc}} = \mathbf{D}_l^{\text{LC}+}. \quad (68)$$

In $\mathbf{D}_l^{\text{LC}+}$, we approximate \mathbf{D}_l using the LC+ approximation [9] for color. Then the second term is

$$\mathbf{D}_l^{\text{soft}} = \mathbf{D}_l - \mathbf{D}_l^{\text{LC}+}. \quad (69)$$

As we see in Appendix A, the LC+ approximation is exact in the limit of collinear emissions [9]. That is, $\mathbf{D}_l - \mathbf{D}_l^{\text{LC}+}$ has no collinear singularity.

This decomposition is important because we can define different treatments of the unresolvable region for the two contributions to \mathbf{D}_l . For splittings derived from $\mathbf{D}_l^{\text{LC}+}$, there are three cuts used to determine when a splitting is unresolvable. First, we impose a fixed infrared cutoff by defining a splitting to be unresolvable whenever $k_\perp^2 < m_\perp^2$, where m_\perp^2 is of order 1 GeV². Second, there is a cut that depends on the energy scale μ_E^2 : a splitting is unresolvable whenever $4z(1-z) < \mu_E^2/Q^2$. Third, there is a cut that depends on μ_C^2 . If $C = \perp$, a splitting is unresolvable whenever $k_\perp^2 < \mu_\perp^2$. If $C = \Lambda$, a splitting is unresolvable whenever $\Lambda^2 < \mu_\Lambda^2$, where Λ^2 is the default ordering variable in DEDUCTOR and is proportional to the virtuality in the splitting. If $C = \angle$, a splitting is unresolvable whenever $\vartheta Q^2 < \mu_\angle^2$ where $\vartheta = [1 - \cos(\theta)]/2$ and θ is the angle between the daughter parton momenta in the rest frame of Q .

We treat splittings derived from $\mathbf{D}_l^{\text{soft}}$ differently. The soft singularity is controlled by the cut $4z(1-z) < \mu_E^2/Q^2$. Since for these splittings there is no collinear singularity, we can omit the cut based on μ_C^2 .

The final ingredient in the formulation presented in this paper is the choice of a path $(\mu_E(t), \mu_C(t))$. The path we choose is has two segments, as shown in Fig. 12. In the first segment, with $0 < t < 1$, μ_C^2 is fixed at Q^2 and μ_E decreases from Q^2 to 0. In the second segment,

with $1 < t < \infty$, μ_E^2 is fixed at 0 and μ_C^2 decreases from Q^2 to 0. In the first path segment, there is no unresolved region available for $\mathcal{D}_l^{\text{LC+}}$ because of the cut imposed by μ_C^2 . However, this cut does not apply for $\mathcal{D}_l^{\text{soft}}$, so there is a contribution from $\mathcal{D}_l^{\text{soft}}$. In the second part, $\mathcal{D}_l^{\text{LC+}}$ contributes, but the unresolved region does not change for $\mathcal{D}_l^{\text{soft}}$, so $\mathcal{D}_l^{\text{soft}}$ does not contribute. This gives Eq. (53) for the complete evolution:

$$\mathcal{U}(\infty, 0) = \mathcal{U}(\infty, 1)\mathcal{U}(1, 0). \quad (70)$$

The second factor here, $\mathcal{U}(\infty, 1)$, is a complete shower using the LC+ approximation for color and either k_T , Λ , or angular ordering. The first factor provides an evolution in parton energy using the soft operator $\mathcal{D}_l^{\text{soft}}$.

In the case of angular ordering, the formulation presented here provides a way to understand an angular ordered shower in which the only cutoff on soft emissions is provided by the fixed cutoff $k_T^2 > m_\perp^2$. If we were to set m_\perp^2 to zero, we would have a naked singularity in the resolved region. With a fixed value of m_\perp^2 , we do not find infinities in the results, but we can find large logarithms, $\log(Q^2/m_\perp^2)$, that are not summed by a renormalization group equation. In the two scale treatment, the large logarithms are absorbed into $\mathcal{U}(1, 0)$.

The LC+ shower provided by $\mathcal{U}(\infty, 1)$ is corrected by the operator $\mathcal{U}(1, 0)$ that is built from $\mathcal{D}_l^{\text{soft}}$, Eq. (69). The splitting operator $\mathcal{D}_l^{\text{soft}}$ has a complicated color structure, making numerical calculations based on this operator difficult. However, this operator tends to be numerically small because it starts with a factor $1/N_c^2 \sim 1/10$ and because it lacks a collinear singularity. Thus one can attack the numerical evaluation by expanding $\mathcal{U}(1, 0)$ in powers of $\mathcal{D}_l^{\text{soft}}$. We have done this in Ref. [14], with splittings according to $\mathcal{D}_l^{\text{soft}}$ interleaved with LC+ evolution. The numerical evidence suggests that an expansion in powers of $\mathcal{D}_l^{\text{soft}}$ is adequate. With the shower formulation presented in this paper, the needed calculations are simpler because $\mathcal{U}(1, 0)$ is applied to the initial hard scattering state, denoted by $|\rho_H\rangle$, which has few partons. The needed calculations are also simpler because the splittings from $\mathcal{D}_l^{\text{soft}}$ do not need to be interleaved with LC+ evolution, which we found to be complicated and computationally expensive.

In the case of e^+e^- annihilation with a color singlet $q\bar{q}$ state $|\rho_H\rangle$ to start the shower, the calculations are, in fact, trivial. Because the space of $q\bar{q}g$ color states is just one dimensional, $\mathcal{D}_l^{\text{soft}}$ applied to $|\rho_H\rangle$ vanishes. Thus $\mathcal{U}(1, 0)|\rho_H\rangle = |\rho_H\rangle$ and no numerical calculation is needed.

Application of the formulation of this paper to hadron-hadron collisions is left to future work. Here, we note that for the Drell-Yan process at the Born level, the initial state with a color singlet $q\bar{q}$ is like a $q\bar{q}$ final state in e^+e^- annihilation, so that $\mathcal{U}(1, 0)|\rho_H\rangle = |\rho_H\rangle$. However, for jet production in hadron-hadron collisions, $\mathcal{U}(1, 0)|\rho_H\rangle \neq |\rho_H\rangle$. Then a perturbative expansion of $\mathcal{U}(1, 0)$ will be needed. However, this expansion should

be much simpler than when powers of $\mathcal{D}_l^{\text{soft}}$ are interleaved with the LC+ shower in the style of Ref. [14].

Finally, we offer the speculation that using multiple scales may prove useful in developing a parton shower algorithm with splitting functions defined at order α_s^2 instead of just α_s . At order α_s^2 , one can have two real emissions, one real emission together with a virtual exchange, or two virtual exchanges. For the case of two real emissions, both can be soft, one can be soft and one collinear with an existing parton, two can be collinear to two existing partons, or two can be collinear with one existing parton. The resulting singular surfaces are much more complicated than they are in a first order shower. It may well be useful to employ different scale parameters to describe an unresolved region that includes all of the singularities.

ACKNOWLEDGMENTS

This work was supported in part by the United States Department of Energy under grant DE-SC0011640. The work benefited from access to the University of Oregon high performance computer cluster, Talapas.

Appendix A: About the Deductor shower

In this appendix, we specify details of the DEDUCTOR shower kinematics [6, 12] and splitting functions [6–9] used in the main text. We adopt a notation that is different from that in Refs. [6–9, 12] and emphasizes some of the features that are important in this paper. We concentrate on the singular operators $\mathcal{D}_l^{[1,0]}(\mu_R^2, \vec{\mu})$ and $\mathcal{D}_l^{[0,1]}(\mu_R^2, \vec{\mu})$ from which the splitting functions used in the shower are derived [1] since these operators carry more information than the shower splitting functions.

1. The form of $\mathcal{D}_l^{[1,0]}$

To define the singular operator for a final state splitting, we begin with the kinematic variables. Before the splitting, there are incoming partons labelled a, b and final state partons $1, 2, \dots, m$. For electron-positron annihilation, the incoming partons do not participate in the shower since they carry no color charge. The final state partons have momenta $\{p\}_m = \{p_1, \dots, p_m\}$ and flavors $\{f\}_m = \{f_1, \dots, f_m\}$. The total momentum of the final state partons is Q . Then also $Q = p_a + p_b$.

Now, for a final state splitting, a parton labelled $l \in \{1, \dots, m\}$ splits. The size of p_l is conveniently described using the auxiliary variable a_l , Eq. (26). It is also useful to define an auxiliary lightlike vector n_l in the plane of p_l and Q , Eq. (23). Parton l splits into a new parton with label l and momentum \hat{p}_l and a new parton with label $m+1$ and momentum \hat{p}_{m+1} . We use a scaled

virtuality variable y , Eq. (24), and a momentum fraction z , Eq. (22), to specify the splitting. We also define an azimuthal angle ϕ of the splitting using the part, k_\perp , of \hat{p}_l that is orthogonal to p_l and n_l . The three splitting variables y , z , and ϕ determine \hat{p}_l and \hat{p}_{m+1} using

$$\begin{aligned}\hat{p}_l &= z h_+(y) p_l + (1-z) h_-(y) n_l + k_\perp, \\ \hat{p}_{m+1} &= (1-z) h_+(y) p_l + z h_-(y) n_l - k_\perp,\end{aligned}\quad (\text{A1})$$

where

$$\begin{aligned}h_\pm(y) &= \frac{1}{2} [1 + y \pm \lambda(y)], \\ \lambda(y) &= \sqrt{(1+y)^2 - 4a_l y}.\end{aligned}\quad (\text{A2})$$

The magnitude of the transverse momentum k_\perp is given by Eq. (27),

$$-\frac{k_\perp^2}{2p_l \cdot Q} = z(1-z)y. \quad (\text{A3})$$

For $i \notin \{l, m+1\}$, the momenta \hat{p}_i are related to the momenta p_i before the splitting by a Lorentz transformation, $\hat{p}_i^\mu = \Lambda_\nu^\mu p_i^\nu$ [6]. This Lorentz transformation is a boost in the plane of p_l and Q and allows $\sum_{i=1}^{m+1} \hat{p}_i = Q$.

For a final state splitting, we need the singular operator $\mathcal{D}_l^{[1,0]}(\mu_R, \vec{\mu})$ that appears in Eqs. (19) and (21). Here μ_R is the renormalization scale and $\vec{\mu}$ is the shower scale, which may have more than one component, as in Eq. (3). The operator $\mathcal{D}_l^{[1,0]}(\mu_R, \vec{\mu})$ has both soft and collinear singularities. We do not now divide it into two parts that get different treatments, as in Eq. (33).

We can now state what $\mathcal{D}_l^{[1,0]}(\mu_R, \vec{\mu})$ contains. We apply $\mathcal{D}_l^{[1,0]}(\mu_R, \vec{\mu})$ to an m -parton state and write the result in the form

$$\begin{aligned}\mathcal{D}_l^{[1,0]}(\mu_R, \vec{\mu}) | \{p, f, c, c'\}_m \rangle \\ = \int d\{\hat{p}, \hat{f}\}_{m+1} | \{\hat{p}, \hat{f}\}_{m+1} \rangle \\ \times \frac{\alpha_s(\mu_R^2)}{2\pi} \hat{D}_l(\{\hat{p}, \hat{f}\}_{m+1}, \{p, f\}_m) | \{c, c'\}_m \rangle.\end{aligned}\quad (\text{A4})$$

Here \hat{D}_l is a function of the momenta and flavors before and after the splitting and is an operator that maps the color space with m final state partons, into the color space with $m+1$ final state partons.

The operator \hat{D}_l has the form derived from Eq. (5.7) of Ref. [9] and Eq. (8.20) of Ref. [6] with dimensional

regulation added,

$$\begin{aligned}\hat{D}_l(\{\hat{p}, \hat{f}\}_{m+1}, \{p, f\}_m; \epsilon) \\ = \left(\frac{\mu_R^2}{2p_l \cdot Q} \right)^\epsilon \frac{(4\pi)^\epsilon}{\Gamma(1-\epsilon)} \int_0^1 dz [z(1-z)]^{-\epsilon} \\ \times \int_0^1 \frac{dy}{y} y^{-\epsilon} [\lambda(y)]^{1-2\epsilon} \theta(\lambda^2(y) > 0) \sum_{\hat{a} \in \mathbb{S}(a)} \\ \times \int \frac{d^{1-2\epsilon}\phi}{S(2-2\epsilon)} \delta(\{\hat{p}, \hat{f}\}_{m+1} - R_l(y, z, \phi, \hat{a}; \{p, f\}_m)) \\ \times \Theta((y, z) \in U(\vec{\mu})) \\ \times \sum_k \frac{1}{2} \left[\theta(k=l) \frac{1}{N(\hat{a}, a)} \hat{P}^{\hat{a}a}(z, y, a_l, \epsilon) \right. \\ \left. - \theta(k \neq l) \delta_{\hat{a}a} \frac{2}{1-z} W_0(\xi_{lk}, a_l, z, y, \phi - \phi_k) \right] \\ \times \{ t_l^\dagger(f_l \rightarrow \hat{f}_l + \hat{f}_{m+1}) \otimes t_k(f_k \rightarrow \hat{f}_k + \hat{f}_{m+1}) \\ + t_k^\dagger(f_k \rightarrow \hat{f}_k + \hat{f}_{m+1}) \otimes t_l(f_l \rightarrow \hat{f}_l + \hat{f}_{m+1}) \}.\end{aligned}\quad (\text{A5})$$

There are dimensionally regulated integrations over splitting variables y , z , and ϕ . The variable ϕ is a unit vector in the $2-2\epsilon$ dimensional transverse momentum space and represents the azimuthal angle of \hat{p}_l around the direction of p_l . The integration over ϕ is an integration over a unit sphere that is a $1-2\epsilon$ dimensional surface. The function $S(2-2\epsilon)$ is the surface area of this sphere, so that

$$\int \frac{d^{1-2\epsilon}\phi}{S(2-2\epsilon)} 1 = 1. \quad (\text{A6})$$

There is also a sum over the flavor \hat{a} of parton l after the splitting, which we use as a splitting variable that specifies the flavor content of the splitting. The set of allowed values of \hat{a} , $\mathbb{S}(a)$, depends on the flavor $a \equiv f_l$ of the parton that splits. For all $a, \hat{a} \in \mathbb{S}(a)$. This corresponds to a splitting $a \rightarrow a + g$, where DEDUCTOR labels the daughter gluon as $m+1$. For $a = g$, also $q \in \mathbb{S}(a)$ for any quark flavor q . This corresponds to a splitting $g \rightarrow q + \bar{q}$, where DEDUCTOR labels the daughter quark as l .

After the integrations, there is a delta function that sets $\{\hat{p}, \hat{f}\}_{m+1}$ to the momenta and flavors obtained from a splitting with variables (y, z, ϕ, \hat{a}) applied to partons with momenta and flavors $\{p, f\}_m$ according to DEDUCTOR conventions.

The idea of the singular operator $\mathcal{D}^{[1,0]}$ is that it integrates over splittings that are arbitrarily close to the soft and collinear limits, but with an ultraviolet cutoff that depends on scale parameters $\vec{\mu}$. The region of (y, z) allowed by the cutoff is called the unresolved region and is denoted by $U(\vec{\mu})$. We therefore insert a theta function that specifies that (y, z) lies in the unresolved region.

DEDUCTOR is a dipole shower. In the following factor, there is a sum over dipole partner partons k . In the first term, the partner parton is the same as the emitting parton, $k = l$. This term contains a color factor $N(\hat{a}, a)$

defined by

$$\begin{aligned} N(q, g) &= T_R, \\ N(q, q) &= C_F, \\ N(g, g) &= C_A, \end{aligned} \quad (\text{A7})$$

where q is any quark or antiquark flavor. Then there is a splitting function $\hat{P}^{\hat{a}a}(z, y, a_l, \epsilon)$. In the case of a $g \rightarrow q\bar{q}$ splitting, where q is a quark flavor, the label l after the splitting is assigned to the quark. Thus we have $a = g$ and $\hat{a} = q$. Then \hat{P}^{qg} is related to the function $\bar{w}_{ll}(\{\hat{p}, \hat{f}\}_{m+1})$ that appears in Eq. (A.1) of Ref. [7] by

$$\frac{4\pi\alpha_s(\mu_R^2)}{y p_l \cdot Q} \frac{\hat{P}^{qg}(z, y, a_l, \epsilon)}{N(q, g)} = \bar{w}_{ll}(\{\hat{p}, \hat{f}\}_{m+1}). \quad (\text{A8})$$

In all other splittings, one of the partons after the splitting is a gluon. The label $m+1$ is assigned to the gluon. Then parton l can be a quark, antiquark, or gluon and $\hat{a} = a$. In this case, \hat{P}^{aa} is related to the functions $\bar{w}_{aa}(\{\hat{p}, \hat{f}\}_{m+1})$ and $\bar{w}_{aa}^{\text{eikonal}}(\{\hat{p}, \hat{f}\}_{m+1})$ that appear in Eqs. (2.23) and (2.58) of Ref. [7] by

$$\begin{aligned} \frac{4\pi\alpha_s(\mu_R^2)}{y p_l \cdot Q} \frac{\hat{P}^{aa}(z, y, a_l, \epsilon)}{N(a, a)} &= \bar{w}_{ll}(\{\hat{p}, \hat{f}\}_{m+1}) - \bar{w}_{ll}^{\text{eikonal}}(\{\hat{p}, \hat{f}\}_{m+1}) \\ &+ \frac{4\pi\alpha_s(\mu_R^2)}{y p_l \cdot Q} \left[\frac{2}{1-z+a_l y} - 2 \right]. \end{aligned} \quad (\text{A9})$$

In Eq. (A8) and Eq. (A9), we calculate \bar{w}_{ll} in $4-2\epsilon$ dimensions by counting the number of spin states of a gluon as $2-2\epsilon$ instead of just 2.

The functions $\hat{P}^{\hat{a}a}(z, y, a_l, \epsilon)$ are somewhat complicated. It is helpful to express these functions using the variables

$$\begin{aligned} x(y) &= \frac{1+y-\lambda(y)}{1+y+\lambda(y)}, \\ \vartheta(y) &= \frac{x(y)}{[z+(1-z)x(y)][1-z+zx(y)]}. \end{aligned} \quad (\text{A10})$$

The variable x vanishes for $y \rightarrow 0$: $x(y) \sim a_l y + \mathcal{O}(y^2)$. The variable ϑ is the angle variable for the splitting defined in Eq. (29). Then we find,

$$\begin{aligned} \hat{P}^{qg}(z, y, a_l, \epsilon) &= T_R \left[1 - \frac{2z(1-z)}{1-\epsilon} \right], \\ \hat{P}^{qq}(z, y, a_l, \epsilon) &= C_F \left[\frac{2}{1-z+a_l y} - 2 + (1-\epsilon)(1-z)h_+(y) \right. \\ &\quad \left. + 2z(1-z) \frac{[h_+(y)-1+x(y)][1-x(y)]}{(1-z+zx(y))^2} \right], \\ \hat{P}^{gg}(z, y, a_l, \epsilon) &= C_A \left[\frac{2}{1-z+a_l y} - 2 \right. \\ &\quad \left. + z(1-z) \left(1 - \frac{2\vartheta(y)[1-\vartheta(y)]}{1-\epsilon} \right) \right]. \end{aligned} \quad (\text{A11})$$

In \hat{P}^{qg} , q can be any flavor of quark, while in \hat{P}^{qq} , q can be any flavor of quark or antiquark. For $\epsilon = 0$, these functions are given in Eqs. (A.1) and (2.23) of Ref. [7] or Appendix B of Ref. [12].

The functions $\hat{P}^{\hat{a}a}(z, y, a_l, \epsilon)$ are simple at $\epsilon = 0, y = 0$:

$$\begin{aligned} \hat{P}^{qg}(z, 0, a_l, 0) &= T_R [1 - 2z(1-z)], \\ \hat{P}^{qq}(z, 0, a_l, 0) &= C_F \frac{1+z^2}{1-z}, \\ \hat{P}^{gg}(z, 0, a_l, 0) &= C_A \left[\frac{2z}{1-z} + z(1-z) \right]. \end{aligned} \quad (\text{A12})$$

The first two of these are the standard DGLAP parton evolution kernels. In \hat{P}^{gg} , both parton l and parton $m+1$ after the splitting are gluons. Parton l carries momentum fraction z , while parton $m+1$ carries momentum fraction $1-z$. The DEDUCTOR algorithm breaks the symmetry between these two gluons. The total probability to produce a gluon with momentum fraction z is given by the standard DGLAP parton evolution kernel,

$$\begin{aligned} \hat{P}^{gg}(z, 0, a_l, 0) + \hat{P}^{gg}(1-z, 0, a_l, 0) &= 2C_A \left[\frac{z}{1-z} + \frac{1-z}{z} + z(1-z) \right]. \end{aligned} \quad (\text{A13})$$

Next in Eq. (A5) is a term proportional to a function $W_0(\xi_{lk}, a_l, z, y, \phi - \phi_k)$. This term comes from interference between emission of a gluon from parton l and emission from dipole partner parton k with $k \neq l$. We write the momentum of parton k before the splitting as

$$\begin{aligned} p_k &= F_{lk} \left[(1 - \xi_{lk}) p_l + \xi_{lk} n_l \right. \\ &\quad \left. + \sqrt{\xi_{lk}(1 - \xi_{lk})Q^2/a_l^2} u_\perp \right]. \end{aligned} \quad (\text{A14})$$

The variable ξ_{lk} is $(1 - \cos \theta_{l,k})/2$ where $\theta_{l,k}$ is the angle between p_k and p_l as measured in the rest frame of Q . The vector u_\perp is a transverse unit vector, $p_l \cdot u_\perp = n_l \cdot u_\perp = 0$ and $u_\perp^2 = -1$. The azimuthal angle of u_\perp is ϕ_k and the azimuthal angle ϕ of k_\perp is defined by

$$k_\perp \cdot u_\perp = -\sqrt{k_T^2} \cos(\phi - \phi_k). \quad (\text{A15})$$

In order to conserve momentum in the splitting, DEDUCTOR makes a small Lorentz transformation on all of the final state momenta except for \hat{p}_l and \hat{p}_{m+1} [6]. This Lorentz transformation changes p_k to

$$\begin{aligned} \hat{p}_k &= F_{lk} \left[e^{\omega(y)}(1 - \xi_{lk}) p_l + e^{-\omega(y)} \xi_{lk} n_l \right. \\ &\quad \left. + \sqrt{\xi_{lk}(1 - \xi_{lk})Q^2/a_l^2} u_\perp \right]. \end{aligned} \quad (\text{A16})$$

The boost angle ω is given by

$$e^{-\omega(y)} = 1 - \sqrt{x(y)y/a_l}. \quad (\text{A17})$$

Thus $\omega(y) \rightarrow 0$ when $y \rightarrow 0$: $\omega(y) \sim y + \mathcal{O}(y^2)$.

The function W_0 is defined by

$$\begin{aligned} & \frac{2}{1-z} W_0(\xi_{lk}, a_l, y, z, \phi - \phi_k) \\ &= \frac{p_l \cdot Q y}{4\pi\alpha_s(\mu_R^2)} A'_{lk}(\{\hat{p}\}_{m+1}) \bar{w}_{lk}^{\text{dipole}}(\{\hat{p}\}_{m+1}) \quad (\text{A18}) \\ & \quad - \left(\frac{2}{1-z+a_ly} - 2 \right). \end{aligned}$$

The function $\bar{w}_{lk}^{\text{dipole}}$ is the familiar dipole radiation function that appears in Ref. [9], Eq. (5.3),

$$\bar{w}_{lk}^{\text{dipole}}(\{\hat{p}\}_{m+1}) = 4\pi\alpha_s(\mu_R^2) \frac{2\hat{p}_l \cdot \hat{p}_k}{\hat{p}_{m+1} \cdot \hat{p}_l \hat{p}_{m+1} \cdot \hat{p}_k}. \quad (\text{A19})$$

This represents the interference between emission of a gluon with momentum \hat{p}_{m+1} from parton l and emission of this gluon from parton k .

To use $\bar{w}_{lk}^{\text{dipole}}$ in a partitioned dipole shower, we multiply by $1 = A'_{lk} + A'_{kl}$, where A'_{lk} is the dipole partitioning function from Ref. [8], Eq. (7.12),

$$\begin{aligned} A'_{lk}(\{\hat{p}\}_{m+1}) &= \frac{\hat{p}_{m+1} \cdot \hat{p}_k \hat{p}_l \cdot Q}{\hat{p}_{m+1} \cdot \hat{p}_k \hat{p}_l \cdot Q + \hat{p}_{m+1} \cdot \hat{p}_l \hat{p}_k \cdot Q}, \quad (\text{A20}) \\ A'_{kl}(\{\hat{p}\}_{m+1}) &= \frac{\hat{p}_{m+1} \cdot \hat{p}_l \hat{p}_k \cdot Q}{\hat{p}_{m+1} \cdot \hat{p}_k \hat{p}_l \cdot Q + \hat{p}_{m+1} \cdot \hat{p}_l \hat{p}_k \cdot Q}. \end{aligned}$$

Then $A'_{lk} \bar{w}_{lk}^{\text{dipole}}$ is associated with emission from parton l and $A'_{kl} \bar{w}_{lk}^{\text{dipole}}$ is associated with emission from parton k . Crucially, $A'_{lk} = 0$ when \hat{p}_{m+1} is collinear with \hat{p}_k , $\hat{p}_{m+1} \cdot \hat{p}_k = 0$. Thus the pole $1/\hat{p}_{m+1} \cdot \hat{p}_k$ in $\bar{w}_{lk}^{\text{dipole}}$ is cancelled. When \hat{p}_{m+1} is collinear with \hat{p}_l , we have $A'_{kl} = 0$ so $A'_{lk} = 1$.

What is $\bar{w}_{lk}^{\text{dipole}}$ when \hat{p}_{m+1} becomes collinear with \hat{p}_l ? This is the limit $\vartheta \rightarrow 0$ with fixed z , or, equivalently, $y \rightarrow 0$ with fixed z . In this limit, we have $A'_{lk} \rightarrow 1$ and

$$\frac{\hat{p}_l \cdot \hat{p}_k}{\hat{p}_{m+1} \cdot \hat{p}_k} \rightarrow \frac{\hat{p}_l \cdot n_l}{\hat{p}_{m+1} \cdot n_l} = \frac{z}{1-z}. \quad (\text{A21})$$

Using $2\hat{p}_{m+1} \cdot \hat{p}_l = 2p_l \cdot Q y$, we find

$$\begin{aligned} & \frac{p_l \cdot Q y}{4\pi\alpha_s(\mu_R^2)} A'_{lk}(\{\hat{p}\}_{m+1}) \bar{w}_{lk}^{\text{dipole}}(\{\hat{p}\}_{m+1}) \\ & \sim \frac{2z}{1-z} = \frac{2}{1-z} - 2 \quad (\text{A22}) \\ & \sim \frac{2}{1-z+a_ly} - 2. \end{aligned}$$

In Eq. (A18), we have subtracted the value of the first line of the right-hand side in this collinear limit.⁸ Thus in the collinear limit, $W_0 \rightarrow 0$.

⁸ Using a denominator $(1-z+a_ly)$ instead of just $(1-z)$ does not change the behavior of the subtraction in the collinear limit, but avoids adding singular behavior that is not present in $A'_{lk} \bar{w}_{lk}^{\text{dipole}}$ in the integration region $(1-z) \ll a_ly \ll 1$. This region corresponds to the emitted soft gluon moving opposite to the mother parton direction.

The function $y A'_{lk} \bar{w}_{lk}^{\text{dipole}}$ is singular in limit of soft emissions, $(1-z) \rightarrow 0$ with fixed ϑ . In this limit, $\hat{p}_{m+1} \sim (1-z) \hat{p}_{m+1}^{(0)}$ with $\hat{p}_{m+1}^{(0)}$ fixed in the soft limit and with $\hat{p}_l \rightarrow p_l$ and $\hat{p}_k \rightarrow p_k$ in the soft limit. One then obtains a result of the form

$$y A'_{lk} \bar{w}_{lk}^{\text{dipole}} = \frac{f(\vartheta)}{1-z} + \mathcal{O}((1-z)^0). \quad (\text{A23})$$

The subtraction in Eq. (A18) eliminates the leading $\vartheta \rightarrow 0$ behavior, leaving

$$\frac{2}{1-z} W_0 = \frac{f(\vartheta) - f(0)}{1-z} + \mathcal{O}((1-z)^0). \quad (\text{A24})$$

Thus W_0 has a finite limit as $(1-z) \rightarrow 0$ at fixed ϑ .

A convenient method to evaluate $W_0(\xi_{lk}, a_l, y, z, \phi - \phi_k)$ is to write the vectors involved as functions of y, z, ϕ and evaluate the vector dot products in Eqs. (A19) and (A20).

Finally in Eq. (A5) there is a factor with color operators. The operator $t_l^\dagger(f_l \rightarrow \hat{f}_l + \hat{f}_{m+1})$, acting on the ket color state $|\{c\}_m\rangle$, gives the new color state $|\{\hat{c}\}_{m+1}\rangle$ that one gets after emitting the new parton $m+1$ from parton l with flavor $f_l = a$, giving a new parton l with flavor $\hat{f}_l = \hat{a}$. This operator is described in some detail in Ref. [6]. Similarly, $t_k(f_k \rightarrow \hat{f}_k + \hat{f}_{m+1})$, acting on the bra color state $\langle\{c'\}_m|$, gives the new color state $\langle\{\hat{c}'\}_{m+1}|$ that one gets after emitting the new parton $m+1$ from parton k with flavor f_k .

In the case that parton $m+1$ is a gluon, the color operators obey the identity

$$\sum_{k=1}^m t_k(f_k \rightarrow f_k + g) = 0. \quad (\text{A25})$$

This identity arises from the fact that the parton color state is an overall color singlet, so that attaching a color generator matrix T_k^c to all of the parton lines k in the state, including $k = l$, gives zero. We have used this identity to add the same term, proportional to $[2/(1-z+a_ly) - 2]$, to both the $k = l$ term and the $k \neq l$ terms in Eq. (A5). We have added this term in both places in order to move the soft \times collinear singularity from the $k \neq l$ terms to the $k = l$ term. After this change, the $k \neq l$ terms, proportional to W_0 , have a soft singularity but not a collinear singularity.

2. The form of $\mathcal{D}_l^{[0,1]}$

As in Eq. (21), the singular operator $\mathcal{D}_l^{[1]}$ associated with parton l consists of two parts, $\mathcal{D}_l^{[1,0]}$ that specifies real splittings of parton l and $\mathcal{D}_l^{[0,1]}$, in which a virtual parton is exchanged. We have described $\mathcal{D}_l^{[1,0]}$. We now would like to define the real part of $\mathcal{D}_l^{[0,1]}(\mu_R, \vec{\mu})$.

This operator comes from virtual graphs, in which we integrate over a momentum q that flows around a

loop. The operator $\mathcal{D}_l^{[0,1]}$ captures the infrared singularities when $q \rightarrow 0$ or q becomes collinear with p_l [1]. Since $\mathcal{D}_l^{[0,1]}$ simply captures the singularities, it is defined to leave parton momenta and flavors unchanged: $\mathcal{D}_l^{[0,1]}|\{p, f, c, c'\}_m\rangle$ is defined to be a linear combination of states $|\{p, f, \hat{c}, c'\}_m\rangle$ with the same momenta and flavors. The operator $\mathcal{D}_l^{[0,1]}$ does, however, change colors. It contains two kinds of terms. First, there are terms with the color structure of self-energy insertions on one of the parton legs. These terms are proportional to the unit operator on the color space. Second, there are terms with the color structure of gluon exchanges between two parton legs, l and k . The gluon line attaches to line l with a color generator matrix T_l^c in the **8**, **3** or $\bar{\mathbf{3}}$ representation according to the flavor of parton l . The gluon line attaches to line k with the appropriate generator matrix T_k^c . Then we sum over the gluon color index c . The result can be denoted by $\mathbf{T}_k \cdot \mathbf{T}_l$. Thus the gluon exchange terms are proportional to either $[\mathbf{T}_k \cdot \mathbf{T}_l \otimes 1]$ for a virtual graph on the ket amplitude or $[1 \otimes \mathbf{T}_k \cdot \mathbf{T}_l]$ for a virtual graph on the bra amplitude. The virtual graphs have $1/\epsilon^2$ and $1/\epsilon$ poles. By using color identities, we can arrange that the terms proportional to the unit operator on the color space have $1/\epsilon^2$ and $1/\epsilon$ poles, while the terms with $[\mathbf{T}_k \cdot \mathbf{T}_l \otimes 1]$ and $[1 \otimes \mathbf{T}_k \cdot \mathbf{T}_l]$ color operators have only $1/\epsilon$ poles that arise from the exchange of a soft gluon.

Since $\mathcal{D}_l^{[0,1]}$ leaves parton momenta and flavors unchanged but can change the m -parton color state, it has the form⁹

$$\begin{aligned} \text{Re } \mathcal{D}_l^{[0,1]}(\mu_R, \vec{\mu})|\{p, f, c, c'\}_m\rangle \\ = |\{p, f\}_m\rangle \frac{\alpha_s(\mu_R^2)}{2\pi} \mathbf{\Gamma}_l(\{p, f\}_m, \epsilon)|\{c, c'\}_m\rangle. \end{aligned} \quad (\text{A26})$$

Now, we need to define $\mathbf{\Gamma}_l$. We will do this by relating $\mathcal{D}_l^{[0,1]}(\mu_R, \vec{\mu})$ to the inclusive splitting probability produced by $\mathcal{D}_l^{[1,0]}(\mu_R, \vec{\mu})$.

The probability associated with a basis state $|\{\hat{p}, \hat{f}, \hat{c}, c'\}_{m+1}\rangle$ is

$$(1|\{\hat{p}, \hat{f}, \hat{c}, c'\}_{m+1}\rangle = (1_{\text{pf}}|\{\hat{p}, \hat{f}\}_{m+1}\rangle)(1_{\text{color}}|\{\hat{c}, c'\}_{m+1}\rangle) \quad (\text{A27})$$

with

$$\begin{aligned} (1_{\text{pf}}|\{\hat{p}, \hat{f}\}_{m+1}\rangle) &= 1, \\ (1_{\text{color}}|\{\hat{c}, c'\}_{m+1}\rangle) &= \langle\{\hat{c}'\}_{m+1}|\{\hat{c}\}_{m+1}\rangle. \end{aligned} \quad (\text{A28})$$

Thus the probability corresponding to $\mathcal{D}_l^{[1,0]}$ applied to

the state $|\{p, f, c, c'\}_m\rangle$ is

$$\begin{aligned} (1|\mathcal{D}_l^{[1,0]}(\mu_R, \vec{\mu})|\{p, f, c, c'\}_m\rangle) \\ = \int d\{\hat{p}, \hat{f}\}_{m+1} \frac{\alpha_s(\mu_R^2)}{2\pi} \\ \times (1_{\text{color}}|\hat{\mathbf{D}}_l(z; \{\hat{p}, \hat{f}\}_{m+1}, \{p, f\}_m; \epsilon)|\{c, c'\}_m\rangle). \end{aligned} \quad (\text{A29})$$

We write this using another operator $\hat{\mathbf{P}}_l$ as

$$\begin{aligned} (1|\mathcal{D}_l^{[1,0]}(\mu_R, \vec{\mu})|\{p, f, c, c'\}_m\rangle) \\ = \frac{\alpha_s(\mu_R^2)}{2\pi} (1_{\text{color}}|\hat{\mathbf{P}}_l(\{p, f\}_m; \epsilon)|\{c, c'\}_m\rangle), \end{aligned} \quad (\text{A30})$$

where $(1_{\text{color}}|$ times the operator $\hat{\mathbf{P}}_l$ is

$$\begin{aligned} (1_{\text{color}}|\hat{\mathbf{P}}_l(\{p, f\}_m; \epsilon)|\{c, c'\}_m\rangle) \\ = \left(\frac{\mu_R^2}{2p_l \cdot Q}\right)^\epsilon \frac{(4\pi)^\epsilon}{\Gamma(1-\epsilon)} \int_0^1 dz [z(1-z)]^{-\epsilon} \\ \times \int_0^1 \frac{dy}{y} y^{-\epsilon} [\lambda(y)]^{1-2\epsilon} \theta(\lambda^2(y) > 0) \sum_{\hat{a} \in \mathbb{S}(a)} \\ \times \int \frac{d^{1-2\epsilon}\phi}{S(2-2\epsilon)} \Theta((y, z) \in U(\vec{\mu})) \\ \times \sum_k \frac{1}{2} \left[\theta(k=l) \frac{1}{N(\hat{a}, a)} \hat{P}^{\hat{a}a}(z, y, \epsilon) \right. \\ \left. - \theta(k \neq l) \delta_{\hat{a}a} \frac{2}{1-z} W_0(\xi_{lk}, a_l, z, y, \phi - \phi_k) \right] \\ \times \langle\{c'\}_m|t_k(f_k \rightarrow \hat{f}_k + \hat{f}_{m+1})t_l^\dagger(f_l \rightarrow \hat{f}_l + \hat{f}_{m+1}) \\ + t_l(f_l \rightarrow \hat{f}_l + \hat{f}_{m+1})t_k^\dagger(f_k \rightarrow \hat{f}_k + \hat{f}_{m+1})|\{c\}_m\rangle. \end{aligned} \quad (\text{A31})$$

Here we have used the momentum conserving delta function in $\hat{\mathbf{D}}_l$ to eliminate the integration over $\{\hat{p}, \hat{f}\}_{m+1}$. In the color factor, we have used the instruction in Eq. (A28) to take the trace of

$$\begin{aligned} \sum_{\hat{c}, \hat{c}'} \rho(\{\hat{c}, \hat{c}'\}_{m+1})|\{\hat{c}\}_{m+1}\rangle\langle\{\hat{c}'\}_{m+1}| \\ = t_l^\dagger(f_l \rightarrow \hat{f}_l + \hat{f}_{m+1})|\{c\}_m\rangle\langle\{c'\}_m|t_k(f_k \rightarrow \hat{f}_k + \hat{f}_{m+1}) \end{aligned} \quad (\text{A32})$$

and the analogous color density matrix with $l \leftrightarrow k$.

We can simplify the color here. In the case that $k = l$,

$$t_l(f_l \rightarrow \hat{f}_l + \hat{f}_{m+1})t_l^\dagger(f_l \rightarrow \hat{f}_l + \hat{f}_{m+1}) = N(\hat{a}, a), \quad (\text{A33})$$

where $N(\hat{a}, a)$ is the Casimir eigenvalue (A7) appropriate to the flavor content of the splitting. When $k \neq l$, the emitted parton $m+1$ is always a gluon. Thus for $k \neq l$,

$$\begin{aligned} t_k(f_k \rightarrow \hat{f}_k + \hat{f}_{m+1})t_l^\dagger(f_l \rightarrow \hat{f}_l + g) \\ = t_l(f_l \rightarrow \hat{f}_l + g)t_k^\dagger(f_k \rightarrow \hat{f}_k + g) \\ = \mathbf{T}_k \cdot \mathbf{T}_l. \end{aligned} \quad (\text{A34})$$

⁹ There are imaginary contributions to the virtual graphs in $\mathcal{D}_l^{[0,1]}$, although the imaginary contributions from final state virtual exchanges with a final state emitting parton cancel [9].

These simplifications give us

$$\begin{aligned}
& (1_{\text{color}} | \hat{\mathbf{P}}_l(\{p, f\}_m; \epsilon) | \{c, c'\}_m) \\
&= \left(\frac{\mu_{\text{R}}^2}{2p_l \cdot Q} \right)^\epsilon \frac{(4\pi)^\epsilon}{\Gamma(1-\epsilon)} \int_0^1 dz [z(1-z)]^{-\epsilon} \\
&\quad \times \int_0^1 \frac{dy}{y} y^{-\epsilon} [\lambda(y)]^{1-2\epsilon} \theta(\lambda^2(y) > 0) \\
&\quad \times \int \frac{d^{1-2\epsilon}\phi}{S(2-2\epsilon)} \Theta((y, z) \in U(\vec{\mu})) \\
&\quad \times \left[\sum_{\hat{a} \in \mathbb{S}(a)} \hat{\mathbf{P}}^{\hat{a}a}(z, y, \epsilon) \langle \{c'\}_m | \{c\}_m \rangle \right. \\
&\quad \left. - \sum_{k \neq l} \frac{2}{1-z} W_0(\xi_{lk}, a_l, z, y, \phi - \phi_k) \right. \\
&\quad \left. \times \langle \{c'\}_m | \mathbf{T}_k \cdot \mathbf{T}_l | \{c\}_m \rangle \right]. \tag{A35}
\end{aligned}$$

This specifies $(1_{\text{color}} | \hat{\mathbf{P}}_l(\{p, f\}_m; \epsilon)$ but not the operator $\hat{\mathbf{P}}_l(\{p, f\}_m; \epsilon)$. We need to specify the color content of $\hat{\mathbf{P}}_l(\{p, f\}_m; \epsilon)$. We make a choice that matches the color structure of the virtual exchange operator $\mathcal{D}_l^{[0,1]}$. We note that

$$\begin{aligned}
& \langle \{c'\}_m | \mathbf{T}_k \cdot \mathbf{T}_l | \{c\}_m \rangle \\
&= \text{Tr} [\mathbf{T}_k \cdot \mathbf{T}_l | \{c\}_m \rangle \langle \{c'\}_m |] \\
&= \text{Tr} [| \{c\}_m \rangle \langle \{c'\}_m | \mathbf{T}_k \cdot \mathbf{T}_l]. \tag{A36}
\end{aligned}$$

Thus we can define the color content of $\hat{\mathbf{P}}_l(\{p, f\}_m; \epsilon)$ by

$$\begin{aligned}
& \hat{\mathbf{P}}_l(\{p, f\}_m; \epsilon) \\
&= \left(\frac{\mu_{\text{R}}^2}{2p_l \cdot Q} \right)^\epsilon \frac{(4\pi)^\epsilon}{\Gamma(1-\epsilon)} \int_0^1 dz [z(1-z)]^{-\epsilon} \\
&\quad \times \int_0^1 \frac{dy}{y} y^{-\epsilon} [\lambda(y)]^{1-2\epsilon} \theta(\lambda^2(y) > 0) \\
&\quad \times \int \frac{d^{1-2\epsilon}\phi}{S(2-2\epsilon)} \\
&\quad \times \Theta((y, z) \in U(\vec{\mu})) \\
&\quad \times \left[\sum_{\hat{a} \in \mathbb{S}(a)} \hat{\mathbf{P}}^{\hat{a}a}(z, y, \epsilon) \right. \\
&\quad \left. - \sum_{k \neq l} \frac{2}{1-z} W_0(\xi_{lk}, a_l, z, y, \phi - \phi_k) \right. \\
&\quad \left. \times \frac{1}{2} \{ [\mathbf{T}_k \cdot \mathbf{T}_l \otimes 1] + [1 \otimes \mathbf{T}_k \cdot \mathbf{T}_l] \} \right]. \tag{A37}
\end{aligned}$$

This enables us to define the operator $\mathbf{\Gamma}_l$ that appears in Eq. (A26) for $\text{Re } \mathcal{D}_l^{[0,1]}$. Because of the familiar real-virtual cancellations, poles in $\mathbf{\Gamma}_l(\{p, f\}_m, \epsilon)$ match the

poles in $-\hat{\mathbf{P}}_l(\{p, f\}_m, \epsilon)$:¹⁰

$$\left[\mathbf{\Gamma}_l(\{p, f\}_m, \epsilon) \right]_{\text{poles}} = - \left[\hat{\mathbf{P}}_l(\{p, f\}_m, \epsilon) \right]_{\text{poles}}. \tag{A38}$$

This leaves the finite part of $\mathbf{\Gamma}_l(\{p, f\}_m, \epsilon)$ undefined. It is not evident how to impose an ultraviolet cutoff on the unresolved region for virtual graphs that matches the cutoff that we used for real emission graphs. In Ref. [12] we proposed a method for this. Here, we propose a simpler method that gives the same result. We define

$$\mathbf{\Gamma}_l(\{p, f\}_m, \epsilon) = -\hat{\mathbf{P}}_l(\{p, f\}_m, \epsilon). \tag{A39}$$

Eq. (A39) gives us

$$(1 | \mathcal{D}_l^{[1]} = (1 | \left[\mathcal{D}_l^{[1,0]} + \mathcal{D}_l^{[0,1]} \right] = 0. \tag{A40}$$

This is significant because the shower splitting operators \mathcal{S}_j for a first order shower are defined by Eq. (12),

$$\mathcal{S}_j(\mu_{\text{R}}, \vec{\mu}) = \frac{\partial}{\partial \mu_{s,j}} \mathcal{D}^{[1]}(\mu_{\text{R}}, \vec{\mu}). \tag{A41}$$

This gives us $(1 | \mathcal{S}_j(\mu_{\text{R}}, \vec{\mu}) = 0$. Then the shower evolution operator $\mathcal{U}(t_2, t_1)$, Eq. (15), is probability preserving.¹¹

$$(1 | \mathcal{U}(t_2, t_1) = (1 |. \tag{A42}$$

3. The form of $\mathcal{D}_{l,\text{soft}}^{[1]}$

In the main text, we have used a decomposition, Eq. (32), of $\mathbf{D}_l(\{\hat{p}, \hat{f}\}_{m+1}; \{p, f\}_m)$ into a part with both soft and collinear singularities and a part with only soft singularities:

$$\mathbf{D}_l = \mathbf{D}_l^{\text{sc}} + \mathbf{D}_l^{\text{soft}}. \tag{A43}$$

In Eq. (57), this decomposition was achieved using the LC+ approximation for color:

$$\begin{aligned}
\mathbf{D}_l^{\text{sc}} &= \mathbf{D}_l^{\text{LC+}}, \\
\mathbf{D}_l^{\text{soft}} &= \mathbf{D}_l - \mathbf{D}_l^{\text{LC+}}. \tag{A44}
\end{aligned}$$

The LC+ approximation [9] is simple. To define $\hat{\mathbf{D}}_l^{\text{LC+}}$, we start with $\hat{\mathbf{D}}_l$ in Eq. (A5) and drop some contributions. We keep all of the contributions for $k = l$. In the contributions for $k \neq l$ (for which parton $m+1$ is a gluon), we expand $\langle \{c'\}_m | t_k(f_k \rightarrow f_k + g) \rangle$ and $t_k^\dagger(f_k \rightarrow f_k + g) | \{c\}_m \rangle$ in color basis vectors and retain

¹⁰ For details, see Ref. [36], for example.

¹¹ The situation is more subtle when there are one or two hadrons in the initial state because then the shower evolution involves the evolution of the parton distribution functions [12, 13].

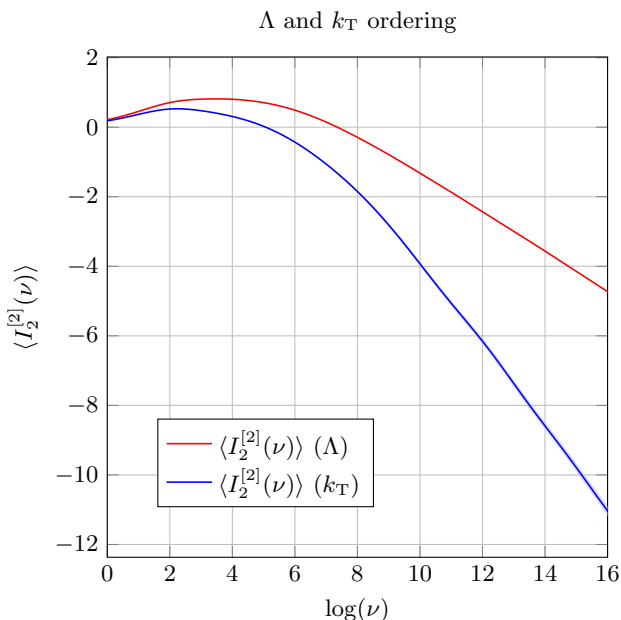


FIG. 18. $\langle I_2^{[2]}(\nu) \rangle$, as in Ref. [18], versus the Laplace parameter ν for the thrust distribution for Λ ordering and k_T ordering.

all contributions in which parton $m+1$ is color connected to parton l , dropping all other contributions.

The corresponding expression for $\hat{P}_l^{\text{LC}+}$ is obtained from \hat{P}_l in Eq. (A37) by retaining the terms proportional to $\hat{P}^{\hat{a}a}(z, y, \epsilon)$ times the unit color matrix. Then for each $k \neq l$ term that was retained in $\hat{D}_l^{\text{LC}+}$, the color matrix $\mathbf{T}_k \cdot \mathbf{T}_l$ is replaced by $C_A/2$ or C_F times the unit color matrix [9].

The result of this is that \hat{D}_l^{soft} and \hat{P}_l^{soft} are given by expressions analogous to the \hat{D}_l and \hat{P}_l that contain only terms proportional to W_0 times color operators. Recall that W_0 has soft singularities but no collinear or soft \times collinear singularities. We conclude that \hat{D}_l^{soft} and \hat{P}_l^{soft} have only soft singularities.

In the formulation of a shower with two scales as presented in the main text, we take $\vec{\mu} = (\mu_E, \mu_C)$, where the collinear sensitive scale μ_C is one of μ_\perp , μ_Λ , or μ_\perp . Then μ_E controls the soft singularity according to Eq. (45). Then for $D_l^{\text{LC}+}$ and $P_l^{\text{LC}+}$, we use the unresolved region $U(\vec{\mu}) = U(\mu_E, \mu_C)$ as defined by Eq. (46). However, for D_l^{soft} and P_l^{soft} , there is no collinear singularity so we can use the unresolved region $U(\mu_E, 0)$ as defined by Eq. (47).

Appendix B: Thrust logarithms for angular ordering

In Fig. 16, we illustrated the application of the methods of this paper to the two jet cross section with the Cambridge algorithm in e^+e^- annihilation. This is quite simple since the contribution from the first component of

the two component path is just the unit operator when one starts with just a $q\bar{q}$ state. A surprising (at least to us) outcome was that with angular ordering for the second component of the path, the results were quite different than with Λ ordering or k_T ordering for the second component.

Although the question of why this is lies outside of the main topic of this paper, we investigate in this appendix whether leaving everything the same in the DEDUCTOR code used for this paper and simply changing from Λ or k_T ordering to angular ordering might change the accuracy with which the shower sums large logarithms.

For this purpose, we consider the thrust distribution, which we had previously investigated [18] (although not with angular ordering). The thrust, T , distribution is strongly peaked at small $1 - T$. It contains a factor $1/(1 - T)$ and large logarithms of $(1 - T)$. To investigate these logarithms, one takes the Laplace transform $\tilde{g}(\nu)$ of the $(1 - T)$ distribution, with Laplace transform variable ν . For large ν , this function contains contributions proportional to $a_s^n \log^k(\nu)$ with $k \leq 2n$. In QCD, $\tilde{g}(\nu)$ exponentiates in the sense that $\log[\tilde{g}(\nu)]$ contains contributions proportional to $a_s^n \log^k(\nu)$ with $k \leq n + 1$. The terms with $k = n + 1$ are the leading-log (LL) terms and the terms with $k = n$ are the next-to-leading-log (NLL) terms. These terms are calculated analytically in Ref. [37]. Ref. [18] provides both analytical and numerical methods for investigating whether a parton shower reproduces those terms. In this appendix, we use one of the numerical methods. We calculate certain quantities $\langle I_n^{[J]}(\nu) \rangle$ that are based on operating J times with the shower splitting operator and calculating its contribution at order α_s^n to $\log[\tilde{g}(\nu)]$ minus what $\log[\tilde{g}(\nu)]$ should be according to the analytic result.

We calculate $\langle I_2^{[2]}(\nu) \rangle$ for the DEDUCTOR splitting functions with exact SU(3) color. In Fig. 18, we show the results with Λ ordering and k_T ordering.¹² This is an order α_s^2 contribution, so the NLL term in the analytical result is proportional to $\log^2(\nu)$. If the parton shower is giving a result correct to NLL, then $\langle I_2^{[2]}(\nu) \rangle$ should *not* contain a $\log^2(\nu)$ contribution for large ν . Thus, for NLL accuracy, the curves representing $\langle I_2^{[2]}(\nu) \rangle$ should be a linear functions of $\log(\nu)$, as indeed they are.

Now we try the same calculation with angular ordering. We display the result in Fig. 19. We see, first, that $\langle I_2^{[2]}(\nu) \rangle$ is much larger in magnitude than the same quantity with Λ ordering, which is shown as a dashed line. This suggests a failure of cancellation of large contributions. For NLL accuracy, $\langle I_2^{[2]}(\nu) \rangle$ should be a linear function of $\log(\nu)$ for large ν but it is not. The blue curve shows $d\langle I_2^{[2]}(\nu) \rangle/d\log(\nu)$. For LL accuracy, this curve

¹² The result in this figure is close that of Figs. 1 and 6 of Ref. [18]. There are small differences because the revised code in this paper treats the running coupling α_s slightly differently from the code in Ref. [18].

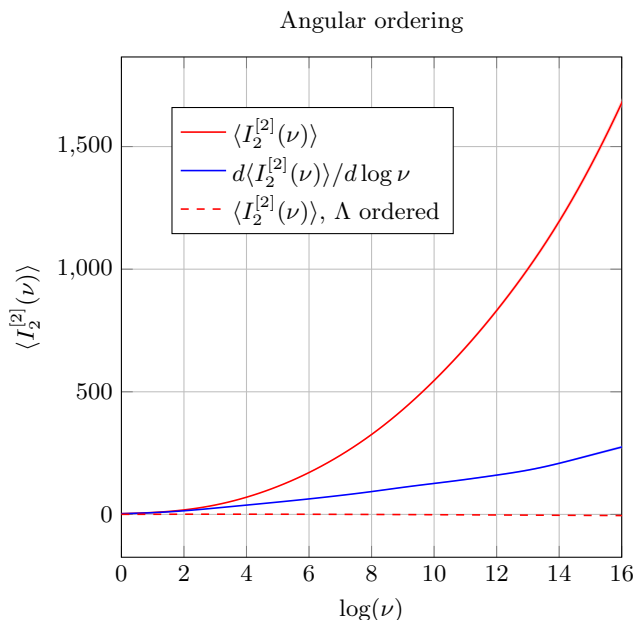


FIG. 19. $\langle I_2^{[2]}(\nu) \rangle$, as in Ref. [18], versus the Laplace parameter ν for the thrust distribution for angular ordering. The Λ -ordered result for $\langle I_2^{[2]}(\nu) \rangle$ is also shown as a dashed line.

should be a linear function of $\log(\nu)$ for large ν . The numerical evidence is perhaps not definitive, but this evidence suggests a failure of the angular ordered shower to achieve LL accuracy. We emphasize that the code for Figs. 18 and 19 is the same except for changing the ordering variable.

-
- [1] Z. Nagy and D. E. Soper, *What is a parton shower?*, *Phys. Rev. D* **98**, 014034 (2018) [INSPIRE].
- [2] M. Bahr *et al.*, *Herwig++ Physics and Manual*, *Eur. Phys. J. C* **58**, 639 (2008) [INSPIRE].
- [3] T. Sjöstrand *et al.*, *An Introduction to PYTHIA 8.2*, *Comput. Phys. Commun.* **191** (2015) 159 [INSPIRE].
- [4] T. Gleisberg, S. Hoeche, F. Krauss, M. Schonherr, S. Schumann, F. Siegert and J. Winter, *Event generation with SHERPA 1.1*, *JHEP* **0902** (2009) 007 [INSPIRE].
- [5] S. Höche and S. Prestel, *The midpoint between dipole and parton showers*, *Eur. Phys. J. C* **75**, 461 (2015) [INSPIRE].
- [6] Z. Nagy and D. E. Soper, *Parton showers with quantum interference*, *JHEP* **0709** (2007) 114 [INSPIRE].
- [7] Z. Nagy and D. E. Soper, *Parton showers with quantum interference: Leading color, spin averaged*, *JHEP* **0803** (2008) 030 [INSPIRE].
- [8] Z. Nagy and D. E. Soper, *Parton showers with quantum interference: Leading color, with spin*, *JHEP* **07**, 025 (2008) [INSPIRE].
- [9] Z. Nagy and D. E. Soper, *Parton shower evolution with subleading color*, *JHEP* **1206** (2012) 044 [INSPIRE].
- [10] Z. Nagy and D. E. Soper, *A parton shower based on factorization of the quantum density matrix*, *JHEP* **1406** (2014) 097 [INSPIRE].
- [11] Z. Nagy and D. E. Soper, *Ordering variable for parton showers*, *JHEP* **1406** (2014) 178 [INSPIRE].
- [12] Z. Nagy and D. E. Soper, *Summing threshold logs in a parton shower*, *JHEP* **1610** (2016) 019 [INSPIRE].
- [13] Z. Nagy and D. E. Soper, *Jets and threshold summation in Deductor*, *Phys. Rev. D* **98**, 014035 (2018) [INSPIRE].
- [14] Z. Nagy and D. E. Soper, *Parton showers with more exact color evolution*, *Phys. Rev. D* **99**, 054009 (2019) [INSPIRE].
- [15] Z. Nagy and D. E. Soper, *Effect of color on rapidity gap survival*, *Phys. Rev. D* **100**, 074012 (2019) [INSPIRE].
- [16] Z. Nagy and D. E. Soper, *Exponentiating virtual imaginary contributions in a parton shower*, *Phys. Rev. D* **100**, 074005 (2019) [INSPIRE].
- [17] Z. Nagy and D. E. Soper, *Evolution of parton showers and parton distribution functions*, *Phys. Rev. D* **102**, 014025 (2020) [INSPIRE].
- [18] Z. Nagy and D. E. Soper, *Summations of large logarithms by parton showers*, *Phys. Rev. D* **104**, 054049 (2021) [INSPIRE].
- [19] G. Marchesini, B. R. Webber, G. Abbiendi, I. G. Knowles, M. H. Seymour and L. Stanco, *HERWIG: A Monte Carlo event generator for simulating hadron emission reactions with interfering gluons. Version 5.1 - April 1991*, *Comput. Phys. Commun.* **67**, 465 (1992) [INSPIRE].
- [20] M. Dasgupta, F. A. Dreyer, K. Hamilton, P. F. Monni, G. P. Salam and G. Soyez, *Parton showers beyond leading logarithmic accuracy*, *Phys. Rev. Lett.* **125**, 052002 (2020) [INSPIRE].
- [21] K. Hamilton, R. Medves, G. P. Salam, L. Scyboz and G. Soyez, *Colour and logarithmic accuracy in final-state parton showers*, *JHEP* **03**, 041 (2021) [INSPIRE].
- [22] I. W. Stewart, F. J. Tackmann and W. J. Waalewijn, *N-Jettiness: An Inclusive Event Shape to Veto Jets*, *Phys. Rev. Lett.* **105**, 092002 (2010) [INSPIRE].
- [23] R. Ángeles Martínez, M. De Angelis, J. R. Forshaw,

- S. Plätzer and M. H. Seymour, *Soft gluon evolution and non-global logarithms*, **JHEP** **05**, 044 (2018) [INSPIRE].
- [24] J. R. Forshaw, J. Holguin and S. Plätzer, *Parton branching at amplitude level*, **JHEP** **08**, 145 (2019) [INSPIRE].
- [25] J. R. Forshaw, J. Holguin and S. Plätzer, *Building a consistent parton shower*, **JHEP** **09**, 014 (2020) [INSPIRE].
- [26] M. De Angelis, J. R. Forshaw and S. Plätzer, *Resummation and Simulation of Soft Gluon Effects beyond Leading Color*, **Phys. Rev. Lett.** **126**, 112001 (2021) [INSPIRE].
- [27] J. Holguin, J. R. Forshaw and S. Plätzer, *Improvements on dipole shower colour*, **Eur. Phys. J. C** **81**, 364 (2021) [INSPIRE].
- [28] S. Höche and D. Reichelt, *Numerical resummation at subleading color in the strongly ordered soft gluon limit*, **Phys. Rev. D** **104**, 034006 (2021) [INSPIRE].
- [29] S. Plätzer and I. Ruffa, *Towards Colour Flow Evolution at Two Loops*, **JHEP** **06**, 007 (2021) [INSPIRE].
- [30] S. Plätzer and M. Sjödal, *Subleading N_c improved Parton Showers*, **JHEP** **07**, 042 (2012) [INSPIRE].
- [31] S. Plätzer, M. Sjödal and J. Thorén, *Color matrix element corrections for parton showers*, **JHEP** **11**, 009 (2018) [INSPIRE].
- [32] J. Isaacson and S. Prestel, *Stochastically sampling color configurations*, **Phys. Rev. D** **99**, 014021 (2019) [INSPIRE].
- [33] Y. L. Dokshitzer, G. D. Leder, S. Moretti and B. R. Webber, *Better jet clustering algorithms*, **JHEP** **08**, 001 (1997) [INSPIRE].
- [34] S. Catani, Y. L. Dokshitzer, F. Fiorani and B. R. Webber, *Average number of jets in e^+e^- annihilation*, **Nucl. Phys. B** **377**, 445-460 (1992) [INSPIRE].
- [35] R. K. Ellis, W. J. Stirling and B. R. Webber, *QCD and collider physics*, Camb. Monogr. Part. Phys. Nucl. Phys. Cosmol. **8**, 1-435 (1996) [INSPIRE].
- [36] Z. Kunszt and D. E. Soper, *Calculation of jet cross-sections in hadron collisions at order α_s^3* , **Phys. Rev. D** **46**, 192 (1992) [INSPIRE].
- [37] S. Catani, L. Trentadue, G. Turnock and B. Webber, *Resummation of large logarithms in e^+e^- event shape distributions*, **Nucl. Phys. B** **407**, 3 (1993) [INSPIRE].